Mathematical Biosciences 296 (2018) 98–112

Contents lists available at ScienceDirect

Mathematical Biosciences

journal homepage: www.elsevier.com/locate/mbs

A Filippov model describing the effects of media coverage and quarantine on the spread of human influenza

Can Chen[a], Nyuk Sian Chong[b], Robert Smith?[*,c]

[a] Department of Mathematics and Physics, College of Science, Zhengzhou University of Aeronautics, Zhengzhou 450015, PR China
[b] School of Informatics and Applied Mathematics, Universiti Malaysia Terengganu, Kuala Terengganu 21030, Malaysia
[c] Department of Mathematics and Faculty of Medicine, University of Ottawa, 585 King Edward Ave, Ottawa, ON K1N 6N5, Canada

ARTICLE INFO

Keywords:
Influenza
Filippov model
Media coverage
Quarantine
Threshold policy
Sliding mode

ABSTRACT

Mass-media reports on an epidemic or pandemic have the potential to modify human behaviour and affect social attitudes. Here we construct a Filippov model to evaluate the effects of media coverage and quarantine on the transmission dynamics of influenza. We first choose a piecewise smooth incidence rate to represent media reports being triggered once the number of infected individuals exceeds a certain critical level I_{c_1}. Further, if the number of infected cases increases and exceeds another larger threshold value I_{c_2} ($> I_{c_1}$), we consider that the incidence rate tends to a saturation level due to the protection measures taken by individuals; meanwhile, we begin to quarantine susceptible individuals when the number of susceptible individuals is larger than a threshold value S_c. Then, for each susceptible threshold value S_c, the global properties of the Filippov model with regard to the existence and stability of all possible equilibria and sliding-mode dynamics are examined, as we vary the infected threshold values I_{c_1} and I_{c_2}. We show generically that the Filippov system stabilizes at either the endemic equilibrium of the subsystem or the pseudoequilibrium on the switching surface or the endemic equilibrium $E_c = (S_c, I_{c_2})$, depending on the choice of the threshold values. The findings suggest that proper combinations of infected and susceptible threshold values can maintain the number of infected individuals either below a certain threshold level or at a previously given level.

1. Introduction

Influenza infections are currently some of the most costly and deadly zoonoses due to the virus's pathogenicity and ability to rapidly spread and evolve [1,2]. Further, influenza has been reported as a significant threat to public health around the world because of the risk of zoonotic infections; that is, it has the potential to cause severe disease in people and to adapt to transmit efficiently in human beings [3–5]. Influenza viruses, belonging to the family *Orthomyxoviridae*, are common contagious pathogens that can cause acute respiratory tract illness in humans [6]. Specifically, influenza viruses can be classified into three types, A, B and C, of which type A and C viruses infect humans and many other species, while type B only infects humans and seals [7,8]. According to reactivity with two surface glycoproteins, hemagglutinin (HA) and neuraminidase (NA), influenza A viruses can be further divided into eighteen HA subtypes (H1–H18) and eleven NA subtypes (N1–N11) with a total of 144 subtypes possible, whereas influenza B virus has no subtypes [9,10].

The first reports of avian influenza A in humans (H5N1) emerged from Hong Kong in 1997, which changed people's general belief that avian influenza viruses were non-infectious to human beings. In March 2013, the first human case of influenza A (H7N9) infection was identified in Eastern China. Since that time, over 650 human cases have been reported to the World Health Organization [11,12]. So far, most reported cases have been epidemiologically linked to close contact with either contaminated environment or infected poultry. Nevertheless, some epidemiological investigations have provided evidence that influenza viruses could transmit from person to person [13–15]. For example, the mutations in H5N1 and H7N9 viruses could potentially transmit between human beings [16,17]. Therefore a number of countries have implemented their control strategies to combat and reduce the burden of a possible potential pandemic outbreak, including primarily media coverage, education, increased hygiene, use of protective devices (e.g., face masks) and quarantine.

In order to better understand influenza infections and quantify the efficacy of various control strategies, mathematical modelling studies have been extensively carried out [18–21]. In particular, the impact of media coverage on the spreading and controlling of influenza has gained a substantial amount of attention [22–25]. Media reports on the numbers of infected influenza cases and deaths can greatly affect

* Corresponding author.
E-mail address: rsmith43@uottawa.ca (R. Smith?).

https://doi.org/10.1016/j.mbs.2017.12.002
Received 21 September 2017; Received in revised form 2 December 2017; Accepted 8 December 2017
Available online 19 December 2017

human behaviour and social responses; for example, individual behaviour may range from hand washing or wearing protective masks to avoiding social contact with infected patients, which may consequently lead to a reduction in the transmission rate or effective contact rate of the susceptible individuals. Xiao et al. [26] extended the classical SIR model to a Filippov model by using a piecewise smooth function, depending on both the case number and its rate of change, to evaluate the effect of media coverage and other control strategies (such as quarantine or isolation) on the spread of A/H1N1 influenza in the Shaanxi province of China. They found that media coverage significantly delayed the epidemic's peak and decreased the severity of influenza outbreak. A stochastic, agent-based model was formulated to investigate the effects of mass-media reports in the 2009 H1N1 pandemic, which shows that the variability in some public control measurements can be affected by the report rate and the rate at which individuals relax their healthy behaviours (i.e., media fatigue) [27].

In practice, at the initial stage of human influenza spreading, both the general public and mass media pay little attention to the disease. Generally, mass-media reports and social responses to the information begin to arise only when the number of infected individuals reaches and exceeds a certain threshold level. Thus individuals are encouraged to change their personal behaviours and take precautionary measures against influenza. Meanwhile, health-education campaigns and hygiene practices can be strengthened through the media to inform the public on current health issues. Nevertheless, with the influenza spreading further, when the number of infected cases increases and exceeds a certain larger threshold level, the incidence rate tends to a saturation level because of the protection measures taken by human beings. Additionally, quarantine (of susceptible individuals) is one of the effective control strategies to reduce the spread of influenza in given populations. Implementing this strategy, however, can inflict significant socio-economic and psychological costs. Consequently, it is important for policymakers to consider when to take this control measure. Thus an appropriate threshold policy is required to combat the influenza outbreak or at least reduce the number of infected individuals to a tolerance level. Therefore our main purpose is to construct a Filippov model to describe the impact of media coverage and quarantine on the transmission dynamics of human influenza by introducing piecewise continuous functions.

2. The Filippov model

In this section, we formulate a Filippov influenza model incorporating media coverage and quarantine of susceptible individuals. Influenza is considered to be manageable when the number of infected individuals is less than an infected threshold level I_{c_1}; thus no control strategy is required. Once the case number is larger than the threshold value I_{c_1}, mass media begins to report information about the disease — including methods of transmission and the numbers of infected cases and deaths — and thus the general public are sufficiently aware of the infection to change their personal behaviours, resulting in a reduction (ϵ_1) in the transmission rate β. Furthermore, when the number of infected individuals increases and exceeds another larger infected threshold value I_{c_2} ($> I_{c_1}$), the incidence rate tends to a saturation level due to healthy measurements taken by the susceptible individuals. We model such an incidence rate with a saturated function (increasing and bounded, $\frac{\beta(1-\epsilon_2)SI}{1+hI}$). Here ϵ_2 is the reduction in the transmission rate β, with $\epsilon_2 > \epsilon_1$, and h measures the inhibitory effort so that $\frac{1}{1+hI}$ describes the saturation due to the protection measures of susceptible individuals or the crowding of infected individuals when the number of infected cases increases. Additionally, when $I > I_{c_2}$, we consider that quarantine of susceptible individuals is not implemented when the number of susceptible individuals is less than a susceptible threshold value S_c, and we quarantine susceptible individuals at a rate of q when $S > S_c$. We illustrate the threshold policy in Fig. 1.

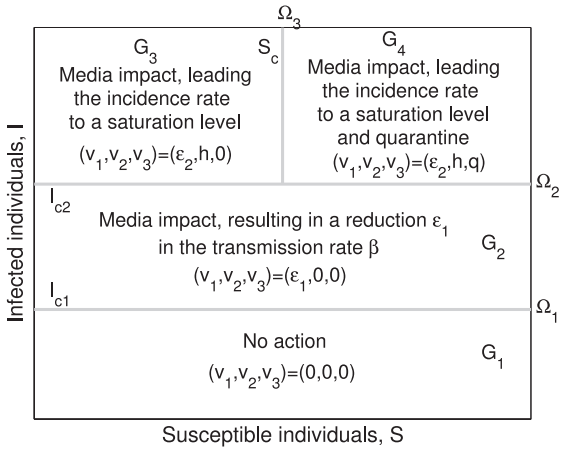

Fig. 1. Schematic diagram illustrating the threshold policy.

We divide the total population into three sub-populations, according to their disease status: susceptible individuals (S), infected individuals (I) and recovered individuals (R). Let Λ be the (constant) recruitment rate to the susceptible population, μ be the natural death rate, α be the disease-related death rate and γ be the recovery rate. Moreover, the detailed descriptions of all these parameters are listed in Table 1. Then we consider the global dynamics of the three sub-populations by constructing a Filippov model, which can be described by

$$\begin{aligned} S' &= \Lambda - \frac{\beta(1-v_1)SI}{1+v_2 I} - \mu S - v_3 S, \\ I' &= \frac{\beta(1-v_1)SI}{1+v_2 I} - \mu I - \alpha I - \gamma I, \\ R' &= \gamma I - \mu R, \end{aligned} \tag{2.1}$$

with

$$(v_1, v_2, v_3) = \begin{cases} (0, 0, 0) & \text{for } I < I_{c_1}, \\ (\epsilon_1, 0, 0) & \text{for } I_{c_1} < I < I_{c_2}, \\ (\epsilon_2, h, 0) & \text{for } S < S_c \text{ and } I > I_{c_2}, \\ (\epsilon_2, h, q) & \text{for } S > S_c \text{ and } I > I_{c_2}. \end{cases} \tag{2.2}$$

Since R (recovered individuals) is not involved in the rest of the equations, we do not include the last equation of model (2.1) in our analysis. Then the (S, I) space $\mathbb{R}^2_+$ can be divided into the following seven regions.

Table 1
Definitions of parameters in the Filippov model (2.1)–(2.2).

Parameter	Description	Value	Resource
Λ	Human recruitment rate (individuals per day)	$\frac{1000}{365}$	[28]
β	Transmission rate (per individual per day)	0.078	[29]
μ	Natural death rate (per day)	$\frac{1}{70\times 365}$	[30]
α	Disease-related death rate (per day)	0.077	[29]
γ	Recovery rate (per day)	0.091	[29]
ϵ_1	Reduction in transmission due to media coverage	0.6	Assumed
ϵ_2	Reduction in transmission due to media coverage	0.7	Assumed
h	The half saturation rate	0.05	Assumed
q	Quarantine rate (per day)	0.1	Assumed

$$
\begin{aligned}
G_1 &= \{(S, I) \in \mathbb{R}^2_+ : I < I_{c_1}\}, \qquad G_2 \\
&= \{(S, I) \in \mathbb{R}^2_+ : I_{c_1} < I < I_{c_2}\}, \\
G_3 &= \{(S, I) \in \mathbb{R}^2_+ : S < S_c \text{ and } I > I_{c_2}\}, \\
G_4 &= \{(S, I) \in \mathbb{R}^2_+ : S > S_c \text{ and } I > I_{c_2}\}, \\
\Omega_1 &= \{(S, I) \in \mathbb{R}^2_+ : I = I_{c_1}\}, \qquad \Omega_2 = \{(S, I) \in \mathbb{R}^2_+ : I = I_{c_2}\}, \\
\Omega_3 &= \{(S, I) \in \mathbb{R}^2_+ : S = S_c \text{ and } I > I_{c_2}\}.
\end{aligned}
$$

The dynamics in region G_i are governed by F_i, for $i = 1, 2, 3, 4$, where

$$
\begin{aligned}
\begin{pmatrix} S' \\ I' \end{pmatrix} &= F_1(S, I) = \begin{pmatrix} \Lambda - \beta SI - \mu S \\ \beta SI - \mu I - \alpha I - \gamma I \end{pmatrix}, && (S, I) \in G_1 \\
\begin{pmatrix} S' \\ I' \end{pmatrix} &= F_2(S, I) = \begin{pmatrix} \Lambda - \beta(1-\epsilon_1) SI - \mu S \\ \beta(1-\epsilon_1) SI - \mu I - \alpha I - \gamma I \end{pmatrix}, && (S, I) \in G_2 \\
\begin{pmatrix} S' \\ I' \end{pmatrix} &= F_3(S, I) = \begin{pmatrix} \Lambda - \frac{\beta(1-\epsilon_2)SI}{1+hI} - \mu S \\ \frac{\beta(1-\epsilon_2)SI}{1+hI} - \mu I - \alpha I - \gamma I \end{pmatrix}, && (S, I) \in G_3 \\
\begin{pmatrix} S' \\ I' \end{pmatrix} &= F_4(S, I) = \begin{pmatrix} \Lambda - \frac{\beta(1-\epsilon_2)SI}{1+hI} - \mu S - qS \\ \frac{\beta(1-\epsilon_2)SI}{1+hI} - \mu I - \alpha I - \gamma I \end{pmatrix}, && (S, I) \in G_4.
\end{aligned}
$$

In addition, the normal vector that is perpendicular to Ω_1 and Ω_2 is defined as $n_1 = (0, 1)^T$, while the normal vector that is perpendicular to Ω_3 is $n_2 = (1, 0)^T$. The following definitions of several types of equilibria for the Filippov system (2.1)–(2.2) are necessary throughout the paper. Denote the right-hand side of the Filippov model (2.1) by f.

Definition 2.1. Let E^* be such that $F_i(E^*) = 0$, $i = 1, 2, 3, 4$. Then E^* is called a *real equilibrium* of system (2.1)–(2.2) if it belongs to G_i and a *virtual equilibrium* if it belongs to G_j, $j \neq i$.

Definition 2.2. A *sliding mode* exists if there are subsets Σ of the manifold Ω_j $(j = 1, 2, 3)$ such that the flows of f (outside Ω_j) are directed toward each other on them.

For our model, $\{(S, I) \in \Omega_1 : \langle n_1, F_1\rangle > 0, \langle n_1, F_2\rangle < 0\}$, $\{(S, I) \in \Omega_2 : \langle n_1, F_2\rangle > 0, \langle n_1, F_3\rangle < 0\}$ and $\{(S, I) \in \Omega_3 : \langle n_2, F_3\rangle > 0, \langle n_2, F_4\rangle < 0\}$ are the sliding modes on Ω_1, Ω_2 and Ω_3, respectively.

By the Filippov convex method [31,32], the differential equations of sliding-mode dynamics on $\Sigma \subset \Omega_j$ can be obtained. We denote them by $\Psi_j(S, I)$. Let $F_+(S, I) = \lim_{(x,y)\to(S,I)} F(x, y)$ for (x, y) on the one side of Ω_j and $F_-(S, I) = \lim_{(x,y)\to(S,I)} F(x, y)$ for (x, y) on the other side of Ω_j. Then $\Psi_j(S, I) = \lambda_j F_+(S, I) + (1 - \lambda_j) F_-(S, I)$, where $\lambda_j = \frac{\langle n, F_-(S,I)\rangle}{\langle n, F_-(S,I) - F_+(S,I)\rangle}$, $0 < \lambda_j < 1$ and n is the normal vector to Ω_j.

Definition 2.3. A point E^P is called a *pseudoequilibrium* if E^P is an equilibrium on the sliding domain Σ; that is, $\Psi_j(E^P) = 0$ and $E^P \in \Sigma \subset \Omega_j$ $(j = 1, 2, 3)$.

Definition 2.4. The set of all points (S, I) on Ω_j $(j = 1, 2, 3)$ such that the flow of f (outside Ω_j) approaches (S, I) from all sides is an *attraction sliding mode*. When the attraction sliding mode consists of only one point, we call this point a *pseudoattractor*.

2.1. Dynamics in region G_i, $i = 1, 2, 3, 4$

In this section, we investigate the dynamics of system (2.1) in region G_i, $i = 1, 2, 3, 4$. Since these systems have been studied in many papers [19,21,23,33], we only present the main results here. For each region G_i, there are two equilibria: the disease-free equilibrium, E_{i0}, and a unique endemic equilibrium, $E_i = (S_i^*, I_i^*)$, $i = 1, 2, 3, 4$, which can be represented as

$$
E_{10} = \left(\frac{\Lambda}{\mu}, 0\right), \quad E_{20} = \left(\frac{\Lambda}{\mu}, 0\right),
$$
$$
E_{30} = \left(\frac{\Lambda}{\mu}, 0\right), \quad E_{40} = \left(\frac{\Lambda}{\mu + q}, 0\right)
$$

and

$$
\begin{aligned}
E_1 &= (S_1^*, I_1^*) = \left(\frac{\mu + \alpha + \gamma}{\beta}, \frac{\Lambda\beta - \mu(\mu + \alpha + \gamma)}{\beta(\mu + \alpha + \gamma)}\right), \\
E_2 &= (S_2^*, I_2^*) = \left(\frac{\mu + \alpha + \gamma}{\beta(1-\epsilon_1)}, \frac{\Lambda\beta(1-\epsilon_1) - \mu(\mu + \alpha + \gamma)}{\beta(1-\epsilon_1)(\mu + \alpha + \gamma)}\right), \\
E_3 &= (S_3^*, I_3^*) = \left(\frac{\Lambda h + \mu + \alpha + \gamma}{\beta(1-\epsilon_2) + \mu h}, \frac{\Lambda\beta(1-\epsilon_2) - \mu(\mu + \alpha + \gamma)}{(\beta(1-\epsilon_2) + \mu h)(\mu + \alpha + \gamma)}\right), \\
E_4 &= (S_4^*, I_4^*) \\
&= \left(\frac{\Lambda h + \mu + \alpha + \gamma}{\beta(1-\epsilon_2) + (\mu + q)h}, \frac{\Lambda\beta(1-\epsilon_2) - (\mu + q)(\mu + \alpha + \gamma)}{(\beta(1-\epsilon_2) + (\mu + q)h)(\mu + \alpha + \gamma)}\right).
\end{aligned}
$$

Furthermore, in region G_i, the basic reproduction number is R_{0i}, for $i = 1, 2, 3, 4$, where

$$
\begin{aligned}
R_{01} &= \frac{\Lambda\beta}{\mu(\mu + \alpha + \gamma)}, \quad R_{02} = \frac{\Lambda\beta(1-\epsilon_1)}{\mu(\mu + \alpha + \gamma)}, \\
R_{03} &= \frac{\Lambda\beta(1-\epsilon_2)}{\mu(\mu + \alpha + \gamma)}, \quad R_{04} = \frac{\Lambda\beta(1-\epsilon_2)}{(\mu + q)(\mu + \alpha + \gamma)}.
\end{aligned}
$$

Lemma 2.1. *The set* $D_i = \left\{(S, I) \in \mathbb{R}^2_+ : S + I \le \frac{\Lambda}{\mu}\right\}$ *is a positively invariant and attracting region for the model in region* G_i, *for* $i = 1, 2, 3$, *while the set* $D_4 = \left\{(S, I) \in \mathbb{R}^2_+ : S + I \le \frac{\Lambda}{\mu + q}\right\}$ *is a positively invariant and attracting region for the model in region* G_4.

Since the proof of Lemma 2.1 is simple and straightforward, we refer the reader to Chong et al. [20,34] for further details.

Theorem 2.1. *The disease-free equilibrium,* E_{i0}, *is globally asymptotically stable if* $R_{0i} < 1$, *while the unique endemic equilibrium,* E_i, *is globally asymptotically stable if* $R_{0i} > 1$, *for* $i = 1, 2, 3, 4$.

Proof. If $R_{0i} < 1$, taking a Lyapunov function $V = \left(S - S_{i0} - S_{i0} \ln \frac{S}{S_{i0}}\right) + I$, where the disease-free equilibrium is $E_{i0} = (S_{i0}, 0)$, we have

$$
\frac{dV}{dt} = -\frac{\mu(S - S_{i0})^2}{S} - (\mu + \alpha + \gamma)(1 - R_{0i})I, \text{ for } i = 1, 2,
$$

and

$$
\begin{aligned}
\frac{dV}{dt} &= -\frac{\mu(S - S_{i0})^2}{S} - (\mu + \alpha + \gamma)\left(1 - \frac{R_{0i}}{1 + hI}\right)I \\
&\le -\frac{\mu(S - S_{i0})^2}{S} - (\mu + \alpha + \gamma)(1 - R_{0i})I, \text{ for } i = 3, 4.
\end{aligned}
$$

When $R_{0i} < 1$, $\frac{dV}{dt} \le 0$ and the equality holds only for $S = S_{i0}$ and $I = 0$. Hence, by LaSalle's invariance principle, E_{i0} is globally asymptotically stable, for $i = 1, 2, 3, 4$.

If $R_{0i} > 1$, the Jacobian matrix of the model in region G_i at the endemic equilibrium E_i possesses two eigenvalues with negative real parts, so it is locally asymptotically stable. Denote the first and second components of the right-hand side of the system in region G_i by $F_{i1}(x)$ and $F_{i2}(x)$, for $i = 1, 2, 3, 4$. Further, choosing a Dulac function $B = 1/(SI)$, we have

$$
\frac{\partial(BF_{i1})}{\partial S} + \frac{\partial(BF_{i2})}{\partial I} = -\frac{\Lambda}{S^2 I} < 0, \text{ for } i = 1, 2,
$$

and

$$
\frac{\partial(BF_{i1})}{\partial S} + \frac{\partial(BF_{i2})}{\partial I} = -\frac{\Lambda}{S^2 I} - \frac{\beta(1-\epsilon_2)h}{(1 + hI)^2} < 0, \text{ for } i = 3, 4.
$$

Thus by the Bendixson–Dulac criterion, we can exclude the existence of limit cycles, and hence E_i is globally asymptotically stable, for $i = 1, 2, 3, 4$. □

2.2. Sliding modes on Ω_1, Ω_2 and their dynamics

In this section, we study the sliding-mode dynamics on the two switching surfaces Ω_1 and Ω_2. First, the existence of the sliding mode on Ω_1 is assured if $\langle n_1, F_1\rangle > 0$ and $\langle n_1, F_2\rangle < 0$. Therefore the sliding mode Σ_1 on Ω_1 is defined as

$$\Sigma_1 = \{(S, I) \in \Omega_1 \colon S_1^* < S < S_2^*\}. \tag{2.3}$$

We use the Filippov convex method [31,32] as follows:

$$\begin{pmatrix} S' \\ I' \end{pmatrix} = \lambda_1 F_1 + (1-\lambda_1)F_2, \text{ where } \lambda_1 = \frac{\langle n_1, F_2\rangle}{\langle n_1, F_2 - F_1\rangle}.$$

Thus we can get differential equations describing the sliding-mode dynamics along the manifold Σ_1 for system (2.1)–(2.2) as

$$\begin{pmatrix} S' \\ I' \end{pmatrix} = \begin{pmatrix} \Lambda - \mu S - (\mu+\alpha+\gamma)I_{c_1} \\ 0 \end{pmatrix}. \tag{2.4}$$

System (2.4) has a unique equilibrium $E_{s1} = (S_{s1}^*, I_{c_1})$, where $S_{s1}^* = \frac{\Lambda - (\mu+\alpha+\gamma)I_{c_1}}{\mu}$. Then $E_{s1} \in \Sigma_1 \subset \Omega_1$ becomes a pseudoequilibrium for system (2.4) if and only if $S_1^* < S_{s1}^* < S_2^*$; that is, $I_2^* < I_{c_1} < I_1^*$. Furthermore, it is stable on $\Sigma_1 \subset \Omega_1$.

Theorem 2.2. *E_{s1} is a stable pseudoequilibrium on $\Sigma_1 \subset \Omega_1$ if it is feasible.*

Proof. We have

$$\frac{\partial}{\partial S}(\Lambda - \mu S - (\mu+\alpha+\gamma)I_{c_1})\Big|_{E_{s1}} = -\mu < 0.$$

Thus solutions are attracting. □

Next, from $\langle n_1, F_2\rangle > 0$ and $\langle n_1, F_3\rangle < 0$, there may exist a sliding mode on Ω_2, depending on the threshold value S_c, which is defined as

$$\Sigma_2 = \{(S, I) \in \Omega_2 \colon S_2^* < S < \min\{S_c, H_1\}\},$$
$$\text{where } H_1 = \frac{(1+hI_{c_2})(\mu+\alpha+\gamma)}{\beta(1-\epsilon_2)}. \tag{2.5}$$

Then if the sliding mode Σ_2 exists, by the Filippov convex method, the sliding-mode dynamics on $\Sigma_2 \subset \Omega_2$ are governed by

$$\begin{pmatrix} S' \\ I' \end{pmatrix} = \begin{pmatrix} \Lambda - \mu S - (\mu+\alpha+\gamma)I_{c_2} \\ 0 \end{pmatrix}. \tag{2.6}$$

There is a unique equilibrium $E_{s2} = (S_{s2}^*, I_{c_2})$ for system (2.6), where $S_{s2}^* = \frac{\Lambda - (\mu+\alpha+\gamma)I_{c_2}}{\mu}$.

Similarly, from $\langle n_1, F_2\rangle > 0$ and $\langle n_1, F_4\rangle < 0$, there may also exist a sliding mode on Ω_2, depending on the threshold value S_c, which is defined as

$$\Sigma_3 = \{(S, I) \in \Omega_2 \colon \max\{S_2^*, S_c\} < S < H_1\}. \tag{2.7}$$

Moreover, if the sliding mode Σ_3 exists, the sliding-mode dynamics on $\Sigma_3 \subset \Omega_2$ are described by

$$\begin{pmatrix} S' \\ I' \end{pmatrix} = \begin{pmatrix} \Lambda - \mu S - (\mu+\alpha+\gamma)I_{c_2} - q(1+hI_{c_2})\frac{\beta(1-\epsilon_1)S - (\mu+\alpha+\gamma)}{\beta(1-\epsilon_1)(1+hI_{c_2}) - \beta(1-\epsilon_2)} \\ 0 \end{pmatrix}. \tag{2.8}$$

System (2.8) has a unique equilibrium $E_{s3} = (S_{s3}^*, I_{c_2})$, where

$$S_{s3}^* = \frac{\begin{array}{c}(\Lambda - (\mu+\alpha+\gamma)I_{c_2})(\beta(1-\epsilon_1)(1+hI_{c_2}) - \beta(1-\epsilon_2)) \\ + q(\mu+\alpha+\gamma)(1+hI_{c_2})\end{array}}{\mu(\beta(1-\epsilon_1)(1+hI_{c_2}) - \beta(1-\epsilon_2)) + q\beta(1-\epsilon_1)(1+hI_{c_2})}.$$

Finally, according to (2.5) and (2.7), we consider different situations of the sliding mode Σ_2 and Σ_3 and seek conditions under which E_{s2} and E_{s3} become pseudoequilibria on $\Sigma_2 \subset \Omega_2$ and $\Sigma_3 \subset \Omega_2$, respectively.

Proposition 2.1. *Note that $H_1 > S_2^*$ is always satisfied. According to the value of S_c, we have the following three situations.*

(I) *If $S_c < S_2^*$, then Σ_2 does not exist, while $\Sigma_3 = \{(S, I) \in \Omega_2 \colon S_2^* < S < H_1\}$ exists.*
- *E_{s2} does not exist, while $E_{s3} \in \Sigma_3 \subset \Omega_2$ if $S_2^* < S_{s3}^* < H_1$; that is, $I_4^* < I_{c_2} < I_2^*$.*

(II) *If $S_2^* < S_c < H_1$, then $\Sigma_2 = \{(S, I) \in \Omega_2 \colon S_2^* < S < S_c\}$, $\Sigma_3 = \{(S, I) \in \Omega_2 \colon S_c < S < H_1\}$.*
- *$E_{s2} \in \Sigma_2 \subset \Omega_2$ if $S_2^* < S_{s2}^* < S_c$; that is, $g_1 < I_{c_2} < I_2^*$, where $g_1 = \frac{\Lambda - \mu S_c}{\mu+\alpha+\gamma}$;*
- *$E_{s3} \in \Sigma_3 \subset \Omega_2$ if $S_c < S_{s3}^* < H_1$; that is, $I_4^* < I_{c_2} < g_3$, where $g_2 = \frac{\Lambda - (\mu+q)S_c}{\mu+\alpha+\gamma} < g_3 < g_1$.*

(III) *If $S_c > H_1$, then $\Sigma_2 = \{(S, I) \in \Omega_2 \colon S_2^* < S < H_1\}$, while the sliding mode Σ_3 does not exist.*
- *$E_{s2} \in \Sigma_2 \subset \Omega_2$ if $S_2^* < S_{s2}^* < H_1$; that is, $I_3^* < I_{c_2} < I_2^*$, while E_{s3} does not exist.*

Proof. We will derive g_3, since all others can be obtained by direct calculation. For situation (II), $S_2^* < S_c < H_1$; thus E_{s3} becomes a pseudoequilibrium on $\Sigma_3 \subset \Omega_2$ if $S_c < S_{s3}^* < H_1$. First, we have $S_{s3}^* < H_1 \Leftrightarrow I_{c_2} > I_4^*$. Then we consider $S_{s3}^* > S_c$. Since

$$\begin{aligned} S_{s3}^* - S_c = {} & \frac{(\Lambda - (\mu+\alpha+\gamma)I_{c_2} - (\mu+q)S_c)(\beta(1-\epsilon_1)(1+hI_{c_2}) - \beta(1-\epsilon_2))}{\mu(\beta(1-\epsilon_1)(1+hI_{c_2}) - \beta(1-\epsilon_2)) + q\beta(1-\epsilon_1)(1+hI_{c_2})} \\ & + \frac{q((\mu+\alpha+\gamma)(1+hI_{c_2}) - \beta(1-\epsilon_2)S_c)}{\mu(\beta(1-\epsilon_1)(1+hI_{c_2}) - \beta(1-\epsilon_2)) + q\beta(1-\epsilon_1)(1+hI_{c_2})}, \end{aligned} \tag{2.9}$$

then if $I_{c_2} > g_1$, we have

$$\begin{aligned} S_{s3}^* - S_c &< \frac{q(1+hI_{c_2})\beta(1-\epsilon_1)(S_2^* - S_c)}{\mu(\beta(1-\epsilon_1)(1+hI_{c_2}) - \beta(1-\epsilon_2)) + q\beta(1-\epsilon_1)(1+hI_{c_2})} \\ &< 0; \end{aligned}$$

if $I_{c_2} < g_2$, we have

$$\begin{aligned} S_{s3}^* - S_c &> \frac{q\beta(1-\epsilon_2)(H_1 - S_c)}{\mu(\beta(1-\epsilon_1)(1+hI_{c_2}) - \beta(1-\epsilon_2)) + q\beta(1-\epsilon_1)(1+hI_{c_2})} \\ &> 0. \end{aligned}$$

Since $S_{s3}^* - S_c$ can be regarded as a quadratic function in variable I_{c_2}, based on the intermediate value theorem and the above discussions, there exists a $g_3 \in (g_2, g_1)$ that satisfies $(S_{s3}^* - S_c)|_{I_{c_2}=g_3} = 0$. Hence when $I_{c_2} > g_3$, we have $S_{s3}^* < S_c$; when $I_{c_2} < g_3$, we have $S_{s3}^* > S_c$. Note that we can also give the exact expression of g_3:

$$g_3 = \frac{B + \sqrt{B^2 + 4\beta(1-\epsilon_1)(\mu+\alpha+\gamma)hC}}{2\beta(1-\epsilon_1)(\mu+\alpha+\gamma)h},$$

where $B = \beta(1-\epsilon_1)h(\Lambda - (\mu+q)S_c) - \beta(\epsilon_2 - \epsilon_1)(\mu+\alpha+\gamma) + qh(\mu+\alpha+\gamma)$ and $C = \beta(\epsilon_2 - \epsilon_1)(\Lambda - (\mu+q)S_c) + q(\mu+\alpha+\gamma - \beta(1-\epsilon_2)S_c)$. □

Theorem 2.3. *E_{s2} is a stable pseudoequilibrium on $\Sigma_2 \subset \Omega_2$ if it is feasible.*

Proof. We have

$$\frac{\partial}{\partial S}(\Lambda - \mu S - (\mu+\alpha+\gamma)I_{c_2})\Big|_{E_{s2}} = -\mu < 0.$$

Hence solutions are attracting. □

Theorem 2.4. *E_{s3} is a stable pseudoequilibrium on $\Sigma_3 \subset \Omega_2$ if it is feasible.*

Proof. We have

$$\frac{\partial}{\partial S}\left(\Lambda-\mu S-(\mu+\alpha+\gamma)I_{c_2}-q(1+hI_{c_2})\frac{\beta(1-\epsilon_1)S-(\mu+\alpha+\gamma)}{\beta(1-\epsilon_1)(1+hI_{c_2})-\beta(1-\epsilon_2)}\right)\Big|_{E_{s3}}$$
$$=-\mu-q(1+hI_{c_2})\frac{\beta(1-\epsilon_1)}{\beta(1-\epsilon_1)(1+hI_{c_2})-\beta(1-\epsilon_2)}<0.$$

Thus solutions are attracting. □

2.3. Sliding mode on Ω_3 and its dynamics

This time, we investigate the sliding-mode dynamics on the discontinuous surface Ω_3. From $\langle n_2, F_3\rangle > 0$ and $\langle n_2, F_4\rangle < 0$, we have

$$((\beta(1-\epsilon_2)+\mu h)S_c-\Lambda h)I<\Lambda-\mu S_c \text{ and } ((\beta(1-\epsilon_2)+(\mu+q)h)S_c - \Lambda h)I>\Lambda-(\mu+q)S_c.$$

Theorem 2.5. *According to the value of the threshold S_c,*

(i) *if $S_c \le \frac{\Lambda h}{\beta(1-\epsilon_2)+(\mu+q)h}$, then there is no sliding mode on Ω_3;*

(ii) *if $\frac{\Lambda h}{\beta(1-\epsilon_2)+(\mu+q)h} < S_c \le \frac{\Lambda h}{\beta(1-\epsilon_2)+\mu h}$, then the sliding mode is*

$$\Sigma_4=\{(S,I)\in\Omega_3\colon I>\max\{I_{c_2},B_1\}\},\quad \text{where } B_1=\frac{\Lambda-(\mu+q)S_c}{(\beta(1-\epsilon_2)+(\mu+q)h)S_c-\Lambda h};\tag{2.10}$$

(iii) *if $S_c > \frac{\Lambda h}{\beta(1-\epsilon_2)+\mu h}$, then the sliding mode is*

$$\Sigma_5=\{(S,I)\in\Omega_3\colon \max\{I_{c_2},B_1\}<I<B_2\},\quad \text{where } B_2=\frac{\Lambda-\mu S_c}{(\beta(1-\epsilon_2)+\mu h)S_c-\Lambda h}.\tag{2.11}$$

Furthermore, the sliding-mode dynamics on $\Sigma_4\subset\Omega_3$ or $\Sigma_5\subset\Omega_3$ are governed by

$$\begin{pmatrix}S'\\I'\end{pmatrix}=\begin{pmatrix}0\\ \frac{\beta(1-\epsilon_2)S_cI}{1+hI}-\mu I-\alpha I-\gamma I\end{pmatrix}.\tag{2.12}$$

There is a sliding equilibrium $E_{s4}=(S_c, I^*_{s4})$ for system (2.12), where $I^*_{s4}=\frac{\beta(1-\epsilon_2)S_c-(\mu+\alpha+\gamma)}{h(\mu+\alpha+\gamma)}$. Moreover, E_{s4} becomes a pseudoequilibrium on $\Sigma_4\subset\Omega_3$ or $\Sigma_5\subset\Omega_3$ if $E_{s4}\in\Sigma_4\subset\Omega_3$ or $E_{s4}\in\Sigma_5\subset\Omega_3$. After a simple calculation, we have the following results.

Proposition 2.2. *We have*

$I^*_{s4}>B_1 \Leftrightarrow S_c>S_4^*$ and $I^*_{s4}<B_2\Leftrightarrow S_c<S_3^*$ and $I^*_{s4}>I_{c_2}\Leftrightarrow S_c>H_1$.

Theorem 2.6. *E_{s4} is a stable pseudoequilibrium if it is feasible.*

Proof. We have

$$\frac{\partial}{\partial I}\left(\frac{\beta(1-\epsilon_2)S_cI}{1+hI}-\mu I-\alpha I-\gamma I\right)\Big|_{E_{s4}}=-\frac{\beta(1-\epsilon_2)S_chI^*_{s4}}{(1+hI^*_{s4})^2}<0.$$

Hence solutions are attracting. □

3. Global behaviour in Case A: $S_c < S_2^*$

We aim to address the richness of the dynamics that system (2.1)–(2.2) can exhibit. Note that we only consider $R_{0i} > 1$ to guarantee the existence of the endemic equilibrium E_i in each region G_i; otherwise, the system will stabilize to its disease-free equilibrium E_{i0} for $i = 1, 2, 3, 4$. Since $S_1^* < S_2^* < S_4^* < S_3^*$ and $I_1^* > I_2^* > I_3^* > I_4^*$, we consider all these cases with varied susceptible threshold value S_c and infected threshold levels I_{c_1}, I_{c_2}. Nevertheless, these cases that have similar dynamics will be combined together. For example, the case $S_c < S_1^*$ and $S_1^* < S_c < S_2^*$ will exhibit similar asymptotic behaviour, so we only need to investigate the case $S_c < S_2^*$. Therefore we consider the following cases generated by $S_c < S_2^*$, $S_2^* < S_c < S_4^*$, $S_4^* < S_c < S_3^*$ and $S_c > S_3^*$, with varied infected threshold values I_{c_1} and I_{c_2}. Furthermore, the existence and global stability of all possible equilibria, as well as sliding-mode dynamics, will be examined from one case to another. In addition, we will summarize the main results and describe the biological implication of all these cases at the end of this paper.

In Case A, since $S_c < S_2^*$, we have $E_3 \notin G_3$; thus E_3 is a virtual equilibrium, denoted by E_3^V. Then, from Proposition 2.1, we see that the sliding mode Σ_2 does not exist, while the sliding mode $\Sigma_3 = \{(S, I) \in \Omega_2\colon S_2^* < S < H_1\}$ exists. Furthermore, E_{s3} is a pseudo equilibrium on $\Sigma_3 \subset \Omega_2$ if $I_4^* < I_{c_2} < I_2^*$. Additionally, there may exist a sliding mode on Ω_3; however, E_{s4} is never a pseudoequilibrium even if there is a sliding mode on Ω_3.

Next, equilibria E_1, E_2 and E_4 may be real, while E_{s1} and E_{s3} may be pseudoequilibria on $\Sigma_1 \subset \Omega_1$ and $\Sigma_3 \subset \Omega_2$, depending on the infected threshold values I_{c_1} and I_{c_2}.

3.1. Case A.1: $I_{c_1} < I_4^*$

In this case, E_1 is a virtual equilibrium, denoted by E_1^V. Furthermore, $E_{s1} \notin \Sigma_1 \subset \Omega_1$.

3.1.1. Case A.11: $I_{c_1} < I_{c_2} < I_4^*$

Under these conditions, E_2 is a virtual equilibrium, whereas E_4 is a real equilibrium, denoted by E_2^V and E_4^R, respectively. Moreover, $E_{s3} \notin \Sigma_3 \subset \Omega_2$. We can get the global asymptotic stability of E_4^R by excluding the existence of limit cycles.

Theorem 3.1. *E_4^R is globally asymptotically stable if $S_c < S_2^*$ and $I_{c_1} < I_{c_2} < I_4^*$.*

Proof. Suppose there exists a limit cycle Υ (shown in Fig. 2) that surrounds the real equilibrium E_4^R and the sliding mode Σ_3. Denote $\Upsilon = \Upsilon_1 + \Upsilon_2 + \Upsilon_3 + \Upsilon_4$, where $\Upsilon_i = \Upsilon \cap G_i$, $i = 1, 2, 3, 4$. Let H be the bounded region delimited by Υ and $H_i = H \cap G_i$ for $i = 1, 2, 3, 4$. In particular, denote the right-hand side of the Filippov model (2.1) by $f(x)$, where $f(x) = (f_1(x), f_2(x))$, and denote the first and second components of the right-hand side of the system in region G_i by $F_{i1}(x)$ and $F_{i2}(x)$ for $i = 1, 2, 3, 4$. Let the Dulac function be $D = \frac{1}{SI}$. Then

$$\iint_H\left(\frac{\partial(Df_1)}{\partial S}+\frac{\partial(Df_2)}{\partial I}\right)dSdI=\sum_{i=1}^{4}\iint_{H_i}\left(\frac{\partial(DF_{i1})}{\partial S}+\frac{\partial(DF_{i2})}{\partial I}\right)dSdI,$$

where

$$\sum_{i=1}^{4}\left(\frac{\partial(DF_{i1})}{\partial S}+\frac{\partial(DF_{i2})}{\partial I}\right)=-\frac{4\Lambda}{S^2I}-\frac{2\beta(1-\epsilon_2)h}{(1+hI)^2}<0\ \ \forall\ (S,I)\in\mathbb{R}^2_+.$$

Let $\widetilde{H}_i$ be the region bounded by $\widetilde{\Upsilon}_i$, $\widetilde{P}_i$ and $\widetilde{Q}_i$, where $\widetilde{H}_i$ and $\widetilde{\Upsilon}_i$ depend on

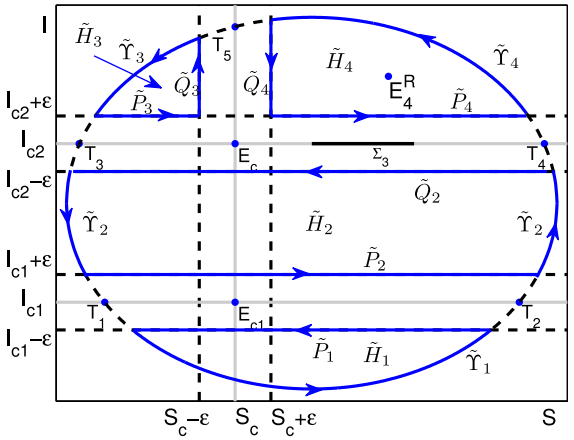

Fig. 2. Schematic diagram illustrating the nonexistence of limit cycles in system (2.1)–(2.2) in Case A.11 when E_4^R is a real equilibrium.

ε and converge to H_i and Υ_i as ε approaches 0. We have

$$\iint_{H_i}\left(\frac{\partial(DF_{i1})}{\partial S}+\frac{\partial(DF_{i2})}{\partial I}\right)dSdI=\lim_{\varepsilon\to 0}\iint_{\widetilde{H}_i}\left(\frac{\partial(DF_{i1})}{\partial S}+\frac{\partial(DF_{i2})}{\partial I}\right)dSdI.$$

Since $dS=F_{11}dt$ and $dI=F_{12}dt$ along $\widetilde{\Upsilon}_1$ and $dI=0$ along $\widetilde{P}_1$, then, by applying Green's theorem to region $\widetilde{H}_1$, we have

$$\begin{aligned}\iint_{\widetilde{H}_1}\left(\frac{\partial(DF_{11})}{\partial S}+\frac{\partial(DF_{12})}{\partial I}\right)dSdI &= \oint_{\partial\widetilde{H}_1} DF_{11}dI-DF_{12}dS\\ &= \int_{\widetilde{\Upsilon}_1} DF_{11}dI-DF_{12}dS+\int_{\widetilde{P}_1} DF_{11}dI\\ &\quad -DF_{12}dS\\ &= -\int_{\widetilde{P}_1} DF_{12}dS.\end{aligned}\tag{3.1}$$

Similarly, we have

$$\iint_{\widetilde{H}_2}\left(\frac{\partial(DF_{21})}{\partial S}+\frac{\partial(DF_{22})}{\partial I}\right)dSdI=-\int_{\widetilde{P}_2} DF_{22}dS-\int_{\widetilde{Q}_2} DF_{22}dS,\tag{3.2}$$

$$\iint_{\widetilde{H}_3}\left(\frac{\partial(DF_{31})}{\partial S}+\frac{\partial(DF_{32})}{\partial I}\right)dSdI=-\int_{\widetilde{P}_3} DF_{32}dS+\int_{\widetilde{Q}_3} DF_{31}dI\tag{3.3}$$

and

$$\iint_{\widetilde{H}_4}\left(\frac{\partial(DF_{41})}{\partial S}+\frac{\partial(DF_{42})}{\partial I}\right)dSdI=-\int_{\widetilde{P}_4} DF_{42}dS+\int_{\widetilde{Q}_4} DF_{41}dI.\tag{3.4}$$

According to (3.1)–(3.4), we have

$$\begin{aligned}0 &> \sum_{i=1}^{4}\iint_{H_i}\left(\frac{\partial(DF_{i1})}{\partial S}+\frac{\partial(DF_{i2})}{\partial I}\right)dSdI\\ &= \lim_{\varepsilon\to 0}\sum_{i=1}^{4}\iint_{\widetilde{H}_i}\left(\frac{\partial(DF_{i1})}{\partial S}+\frac{\partial(DF_{i2})}{\partial I}\right)dSdI\\ &= \lim_{\varepsilon\to 0}\Bigg(-\int_{\widetilde{P}_1} DF_{12}dS-\int_{\widetilde{P}_2} DF_{22}dS-\int_{\widetilde{Q}_2} DF_{22}dS-\int_{\widetilde{P}_3} DF_{32}dS\\ &\quad +\int_{\widetilde{Q}_3} DF_{31}dI\\ &\quad -\int_{\widetilde{P}_4} DF_{42}dS+\int_{\widetilde{Q}_4} DF_{41}dI\Bigg).\end{aligned}\tag{3.5}$$

Denote the intersection points of the closed trajectory Υ and the line $I=I_{c_1}$ (resp. $I=I_{c_2}$) by T_1 and T_2 (T_3 and T_4), and denote the intersection point of Υ and the line $S=S_c$ in the region of $I>I_{c_2}$ by T_5. In addition, denote the intersection point of the line $I=I_{c_1}$ ($I=I_{c_2}$) and the line $S=S_c$ by E_{c_1} (E_c). Note that $T_{11}<S_c<T_{21}$, $T_{31}<S_c<T_{41}$ and $T_{52}>I_{c_2}$. Then the inequality (3.5) becomes

$$\begin{aligned}0 &> -\int_{T_{21}}^{T_{11}}\left(\beta-\frac{\mu+\alpha+\gamma}{S}\right)dS-\int_{T_{11}}^{T_{21}}\left(\beta(1-\epsilon_1)-\frac{\mu+\alpha+\gamma}{S}\right)dS\\ &\quad -\int_{T_{41}}^{T_{31}}\left(\beta(1-\epsilon_1)-\frac{\mu+\alpha+\gamma}{S}\right)dS-\int_{T_{31}}^{S_c}\left(\frac{\beta(1-\epsilon_2)}{1+hI}-\frac{\mu+\alpha+\gamma}{S}\right)dS\\ &\quad -\int_{S_c}^{T_{41}}\left(\frac{\beta(1-\epsilon_2)}{1+hI}-\frac{\mu+\alpha+\gamma}{S}\right)dS\\ &\quad +\int_{I_{c_2}}^{T_{52}}\left(\frac{\Lambda}{SI}-\frac{\beta(1-\epsilon_2)}{1+hI}-\frac{\mu}{I}\right)dI+\int_{T_{52}}^{I_{c_2}}\left(\frac{\Lambda}{SI}-\frac{\beta(1-\epsilon_2)}{1+hI}-\frac{\mu+q}{I}\right)dI\\ &= \beta\epsilon_1(T_{21}-T_{11})+q\ln\left(\frac{T_{52}}{I_{c_2}}\right)+\int_{T_{31}}^{T_{41}}\left(\beta(1-\epsilon_1)-\frac{\beta(1-\epsilon_2)}{1+hI}\right)dS\\ &> \beta\epsilon_1(T_{21}-T_{11})+q\ln\left(\frac{T_{52}}{I_{c_2}}\right)+\frac{\beta(1-\epsilon_2)hI}{1+hI}(T_{41}-T_{31})>0,\end{aligned}$$

which is a contradiction. Therefore, this rules out the existence of the limit cycle Υ surrounding the real equilibrium E_4^R and the sliding domain Σ_3. □

Throughout this paper, parameter values that are used in the numerical simulations are chosen from Table 1. Specifically, these parameter values are selected based on the investigation of the transmission of influenza H7N9. Nevertheless, there is one exception: we fix $\mu=0.06$ so that all figures are of manageable size. Here we use the dotted curves and dash-dot lines to denote the S-nullclines and I-nullclines, respectively, of the system (2.1)–(2.2). First, note that $S=S_1^*$ and $S=S_2^*$ are the I-nullclines of F_1 and F_2, denoted by L_{12} and L_{22}, while the curves $\left\{(S,I)\in G_3\colon I=\frac{\beta(1-\epsilon_2)S-(\mu+\alpha+\gamma)}{(\mu+\alpha+\gamma)h}\right\}$ and $\left\{(S,I)\in G_4\colon I=\frac{\beta(1-\epsilon_2)S-(\mu+\alpha+\gamma)}{(\mu+\alpha+\gamma)h}\right\}$ are the I-nullclines of F_3 and F_4, denoted by L_{32} and L_{42}, respectively. Next, the curves $\left\{(S,I)\in G_1\colon I=\frac{\Lambda-\mu S}{\beta S}\right\}$ and $\left\{(S,I)\in G_2\colon I=\frac{\Lambda-\mu S}{\beta(1-\epsilon_1)S}\right\}$ are the S-nullclines of F_1 and F_2, denoted by L_{11} and L_{21}, whereas the curves $\left\{(S,I)\in G_3\colon I=\frac{\Lambda-\mu S}{(\beta(1-\epsilon_2)+\mu h)S-\Lambda h}\right\}$ and $\left\{(S,I)\in G_4\colon I=\frac{\Lambda-(\mu+q)S}{(\beta(1-\epsilon_2)+(\mu+q)h)S-\Lambda h}\right\}$ are the S-nullclines of F_3 and F_4, denoted by L_{31} and L_{41}, respectively.

Here we choose $S_c=4$, $I_{c_1}=1.5$, $I_{c_2}=3$, to explore the phase portrait for Case A.11. From Fig. 3, we see that all solutions with any initial values in $\mathbb{R}^2_+$ will converge to E_4^R as $t\to\infty$.

3.1.2. Case A.12: $I_4^*<I_{c_2}<I_2^*$

Under these conditions, both E_2 and E_4 are virtual equilibria, denoted by E_2^V and E_4^V, respectively. Furthermore, E_{s3} is a pseudoequilibrium on $\Sigma_3\subset\Omega_2$. Then, using a similar method as in Theorem 3.1 to the proof of the non-existence of limit cycles, we get the following result.

Theorem 3.2. *E_{s3} is globally asymptotically stable if $S_c<S_2^*$ and $I_{c_1}<I_4^*<I_{c_2}<I_2^*$.*

The phase portrait of this case is represented in Fig. 4. All orbits of system (2.1)–(2.2) will converge to E_{s3} as time t increases.

3.1.3. Case A.13: $I_{c_2}>I_2^*$

Under these conditions, E_2 is a real equilibrium, whereas E_4 is a virtual equilibrium, denoted by E_2^R and E_4^V, respectively. Furthermore, $E_{s3}\notin\Sigma_3\subset\Omega_2$. Similarly, by proving the non-existence of limit cycles, we have the following result.

Theorem 3.3. *E_2^R is globally asymptotically stable if $S_c<S_2^*$, $I_{c_1}<I_4^*$ and $I_{c_2}>I_2^*$.*

Fig. 5 shows the phase portrait for this case. All trajectories of system (2.1)–(2.2) will eventually approach E_2^R.

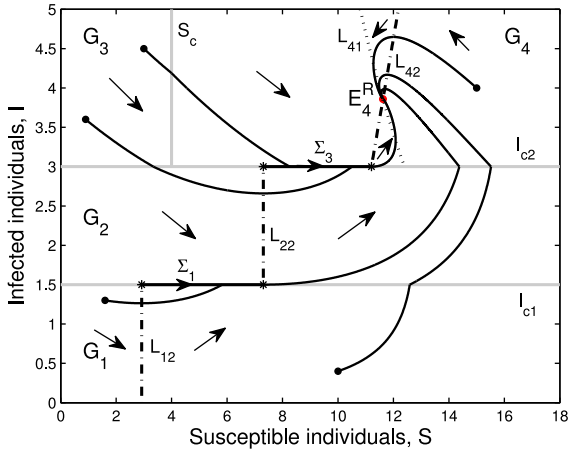

Fig. 3. E_4^R is globally asymptotically stable in Case A.11, where $S_c=4$, $I_{c_1}=1.5$ and $I_{c_2}=3$.

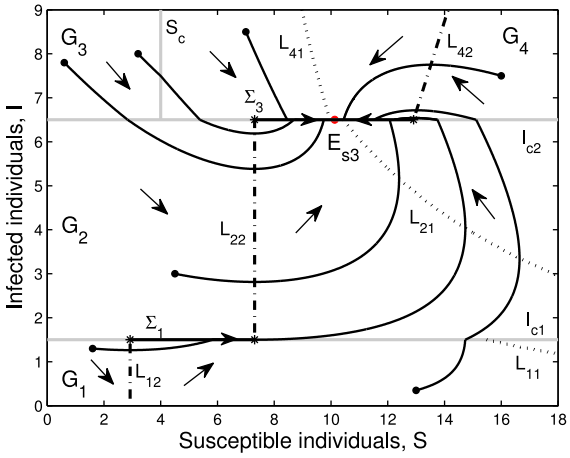

Fig. 4. E_{s3} is globally asymptotically stable in Case A.12, where $S_c = 4$, $I_{c_1} = 1.5$ and $I_{c_2} = 6.5$.

3.2. Case A.2: $I_4^* < I_{c_1} < I_2^*$

In this case, for the situation $I_4^* < I_{c_1} < I_{c_2} < I_2^*$, the analysis is similar to Case A.12 and is not given here; for the situation $I_{c_2} > I_2^*$, the discussion is similar to Case A.13, and we omit it.

3.3. Case A.3: $I_2^* < I_{c_1} < I_1^*$

In this case, E_1, E_2 and E_4 are virtual equilibria, denoted by E_1^V, E_2^V and E_4^V, respectively. Moreover, E_{s1} is a pseudoequilibrium on $\Sigma_1 \subset \Omega_1$.

3.3.1. Case A.31: $I_{c_2} > I_{c_1} > I_2^*$

Under these conditions, $E_{s3} \notin \Sigma_3 \subset \Omega_2$. Thus E_{s1} is the unique equilibrium of system (2.1)–(2.2). Then we have the following result.

Theorem 3.4. *E_{s1} is globally asymptotically stable if $S_c < S_2^*$, $I_2^* < I_{c_1} < I_1^*$ and $I_{c_2} > I_{c_1} > I_2^*$.*

Fig. 6 displays the phase portrait of this case. All solutions of system (2.1)–(2.2) will eventually approach E_{s1}.

3.4. Case A.4: $I_{c_1} > I_1^*$

In this case, E_1 is a real equilibrium, whereas E_2 and E_4 are virtual equilibria, denoted by E_1^R, E_2^V and E_4^V, respectively. Moreover, $E_{s1} \notin \Sigma_1 \subset \Omega_1$.

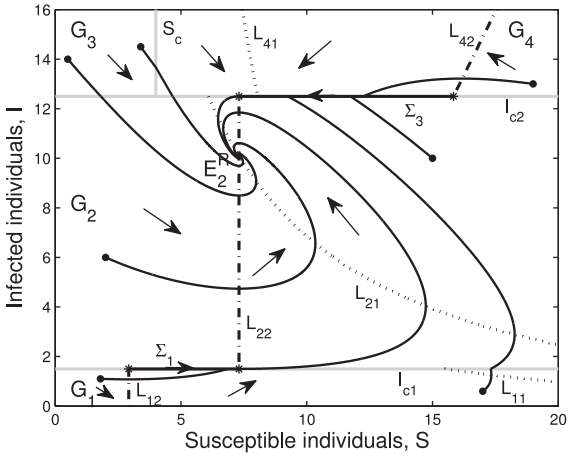

Fig. 5. E_2^R is globally asymptotically stable in Case A.13, where $S_c = 4$, $I_{c_1} = 1.5$ and $I_{c_2} = 12.5$.

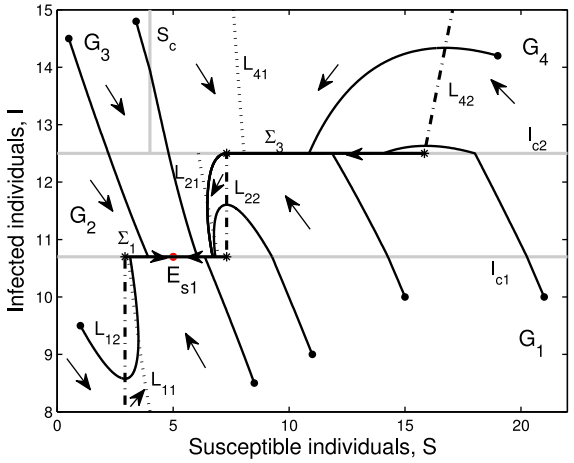

Fig. 6. E_{s1} is globally asymptotically stable in Case A.31, where $S_c = 4$, $I_{c_1} = 10.7$ and $I_{c_2} = 12.5$.

3.4.1. Case A.41: $I_{c_2} > I_{c_1} > I_1^*$

Under these conditions, $E_{s3} \notin \Sigma_3 \subset \Omega_2$. Note that E_1^R is the unique equilibrium of system (2.1)–(2.2). Then we have the following result.

Theorem 3.5. *E_1^R is globally asymptotically stable if $S_c < S_2^*$ and $I_{c_2} > I_{c_1} > I_1^*$.*

The phase portrait of this case is given in Fig. 7. All trajectories of system (2.1)–(2.2) will eventually converge to E_1^R.

4. Global behaviour in Case B: $S_2^* < S_c < S_4^*$

For Case B, E_3 is a virtual equilibrium, denoted by E_3^V. Since $S_2^* < S_c < S_4^*$, we have $I_{s4}^* < I_4^*$ and $I_4^* < g_2 < g_3 < g_1 < I_2^*$. Furthermore, there may exist a sliding mode on Ω_3, whereas E_{s4} is never a pseudoequilibrium even if there exists a sliding mode on Ω_3. Then, from Propositions 2.1 and 2.2, we have the following result.

Proposition 4.1. *In Case B, $S_2^* < S_c < S_4^*$, we have:*

(i) *if $S_c < H_1$, then $\Sigma_2 = \{(S, I) \in \Omega_2 : S_2^* < S < S_c\}$ and $\Sigma_3 = \{(S, I) \in \Omega_2 : S_c < S < H_1\}$. Furthermore, $E_{s2} \in \Sigma_2 \subset \Omega_2$ if $g_1 < I_{c_2} < I_2^*$, whereas $E_{s3} \in \Sigma_3 \subset \Omega_2$ if $I_4^* < I_{c_2} < g_3$;*
(ii) *if $S_c > H_1$, then $\Sigma_2 = \{(S, I) \in \Omega_2 : S_2^* < S < H_1\}$ and the sliding mode Σ_3 does not exist. Moreover, $E_{s2} \in \Sigma_2 \subset \Omega_2$ if $I_3^* < I_{c_2} < I_2^*$.*

Next, E_1, E_2 or E_4 may be real equilibria and E_{s1}, E_{s2} or E_{s3} may become pseudoequilibria, depending on the values of the infected thresholds I_{c_1} and I_{c_2}.

4.1. Case B.1: $I_{c_1} < I_4^*$

In this case, E_1 is a virtual equilibrium, denoted by E_1^V. Furthermore, $E_{s1} \notin \Sigma_1 \subset \Omega_1$.

4.1.1. Case B.11: $I_{c_1} < I_{c_2} < I_4^*$

Under these conditions, E_2 is a virtual equilibrium, whereas E_4 is a real equilibrium, denoted by E_2^V and E_4^R, respectively. Since $I_{s4}^* < I_4^*$ and $I_{c_2} < I_4^*$, from Proposition 4.1, if $I_{c_2} < I_{s4}^*$ (i.e., $S_c > H_1$), we see that $E_{s2} \notin \Sigma_2 \subset \Omega_2$ and the sliding mode Σ_3 does not exist; while if $I_{s4}^* < I_{c_2} < I_4^*$ (i.e., $S_c < H_1$), we have $E_{s2} \notin \Sigma_2 \subset \Omega_2$ and $E_{s3} \notin \Sigma_3 \subset \Omega_2$. Thus there is no pseudoequilibrium on Ω_2. Then we have the following result.

Theorem 4.1. *E_4^R is globally asymptotically stable if $S_2^* < S_c < S_4^*$ and $I_{c_1} < I_{c_2} < I_4^*$.*

The phase portrait of this case is displayed in Fig. 8. All trajectories of system (2.1)–(2.2) will converge to E_4^R.

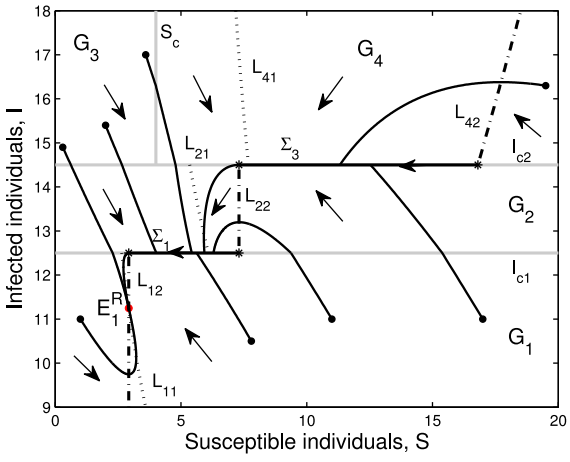

Fig. 7. E_1^R is globally asymptotically stable in Case A.41, where $S_c = 4$, $I_{c_1} = 12.5$ and $I_{c_2} = 14.5$.

4.1.2. Case B.12: $I_4^* < I_{c_2} < I_2^*$

Under these conditions, E_2 and E_4 are virtual equilibria, denoted by E_2^V and E_4^V, respectively. Since $I_{s4}^* < I_4^* < I_{c_2}$, then $H_1 > S_c$. From Proposition 4.1, we can obtain the following results.

Proposition 4.2. *According to the threshold value I_{c_2},*

(i) *if $I_4^* < I_{c_2} < g_3$, we have $E_{s2} \notin \Sigma_2 \subset \Omega_2$, $E_{s3} \in \Sigma_3 \subset \Omega_2$;*
(ii) *if $g_3 < I_{c_2} < g_1$, we have $E_{s2} \notin \Sigma_2 \subset \Omega_2$, $E_{s3} \notin \Sigma_3 \subset \Omega_2$;*
(iii) *if $g_1 < I_{c_2} < I_2^*$, we have $E_{s2} \in \Sigma_2 \subset \Omega_2$, $E_{s3} \notin \Sigma_3 \subset \Omega_2$.*

The phase portraits for Case B.12 are shown in Fig. 9. First, when $I_4^* < I_{c_2} < g_3$, E_{s3} is the unique globally asymptotically stable equilibrium, and all trajectories will converge to E_{s3}, as shown in Fig. 9(A). Next, when $g_3 < I_{c_2} < g_1$, no equilibrium exists for system (2.1)–(2.2), but we see that all orbits will approach the pseudoattractor $E_c = (S_c, I_{c_2})$, as represented in Fig. 9(B). Finally, when $g_1 < I_{c_2} < I_2^*$, E_{s2} becomes the unique globally asymptotically stable equilibrium, and all solutions will approach E_{s2}, as displayed in Fig. 9(C).

4.1.3. Case B.13: $I_{c_2} > I_2^*$

Under these conditions, E_2 is a real equilibrium, whereas E_4 is a virtual equilibrium, denoted by E_2^R and E_4^V, respectively. We also have $H_1 > S_c$. Furthermore, $E_{s2} \notin \Sigma_2 \subset \Omega_2$ and $E_{s3} \notin \Sigma_3 \subset \Omega_2$. Then we have the following result.

Theorem 4.2. *E_2^R is globally asymptotically stable if $S_2^* < S_c < S_4^*$, $I_{c_1} < I_4^*$ and $I_{c_2} > I_2^*$.*

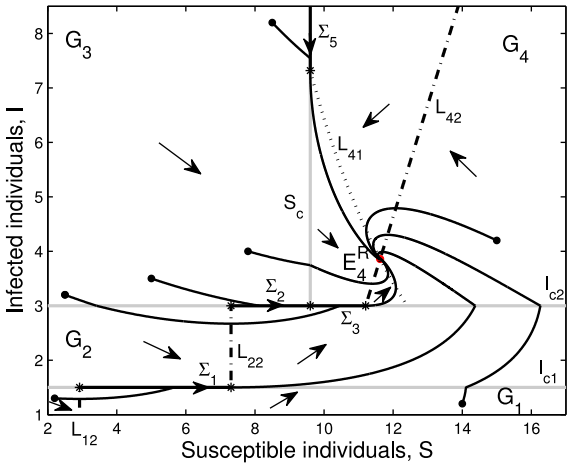

Fig. 8. E_4^R is globally asymptotically stable in Case B.11, where $S_c = 9.6$, $I_{c_1} = 1.5$ and $I_{c_2} = 3$.

Fig. 10 displays the phase portrait of this case. All trajectories will converge to E_2^R.

4.2. Case B.2: $I_4^* < I_{c_1} < I_2^*$

In this case, for the situation $I_4^* < I_{c_1} < I_{c_2} < I_2^*$, the analysis is similar to Case B.12 and is not given here; for the situation $I_{c_2} > I_2^*$, the discussion is similar to Case B.13, and we omit it.

4.3. Case B.3: $I_2^* < I_{c_1} < I_1^*$

In this case, E_1, E_2 and E_4 are virtual equilibria, denoted by E_1^V, E_2^V and E_4^V, respectively. Moreover, E_{s1} is a pseudoequilibrium on $\Sigma_1 \subset \Omega_1$.

4.3.1. Case B.31: $I_{c_2} > I_{c_1} > I_2^*$

Under these conditions, we have $H_1 > S_c$. Furthermore, $E_{s2} \notin \Sigma_2 \subset \Omega_2$ and $E_{s3} \notin \Sigma_3 \subset \Omega_2$. Hence E_{s1} is the unique equilibrium. Then we have the following.

Theorem 4.3. *E_{s1} is globally asymptotically stable if $S_2^* < S_c < S_4^*$, $I_2^* < I_{c_1} < I_1^*$ and $I_{c_2} > I_{c_1} > I_2^*$.*

The phase portrait of this case is represented in Fig. 11. All solutions will converge to E_{s1}.

4.4. Case B.4: $I_{c_1} > I_1^*$

In this case, E_1 is a real equilibrium, whereas E_2 and E_4 are virtual equilibria, denoted by E_1^R, E_2^V and E_4^V, respectively. Moreover, $E_{s1} \notin \Sigma_1 \subset \Omega_1$.

4.4.1. Case B.41: $I_{c_2} > I_{c_1} > I_1^*$

Under these conditions, we also have $H_1 > S_c$. Furthermore, $E_{s2} \notin \Sigma_2 \subset \Omega_2$ and $E_{s3} \notin \Sigma_3 \subset \Omega_2$. Hence E_1^R is the unique equilibrium. Then we have the following result.

Theorem 4.4. *E_1^R is globally asymptotically stable if $S_2^* < S_c < S_4^*$ and $I_{c_2} > I_{c_1} > I_1^*$.*

The phase portrait of this case is shown in Fig. 12. All trajectories will converge to E_1^R.

5. Global behaviour in Case C: $S_4^* < S_c < S_3^*$

For Case C, both E_3 and E_4 are virtual equilibria, denoted by E_3^V and E_4^V, respectively. Since $S_4^* < S_c < S_3^*$, then we have $I_4^* < I_{s4}^* < I_3^*$ and $g_2 < I_4^* < I_3^* < g_1 < I_2^*$. The discussions for the sliding mode Σ_2 and Σ_3, and the pseudoequilibrium E_{s2} and E_{s3} are similar to Proposition 4.1. In addition, from Theorem 2.5, we see that there may exist a sliding mode Σ_4 or Σ_5 on Ω_3, and E_{s4} becomes a pseudoequilibrium if $S_c > H_1$ for Case C.

Next, E_1, E_2 may be real equilibria and E_{s1}, E_{s2} or E_{s3} may become pseudoequilibria, depending on the values of the infected thresholds I_{c_1} and I_{c_2}.

5.1. Case C.1: $I_{c_1} < I_4^*$

In this case, E_1 is a virtual equilibrium, denoted by E_1^V. Furthermore, $E_{s1} \notin \Sigma_1 \subset \Omega_1$.

5.1.1. Case C.11: $I_{c_1} < I_{c_2} < I_4^*$

Under these conditions, E_2 is a virtual equilibrium, denoted by E_2^V. Since $I_{c_2} < I_4^* < I_{s4}^*$, then $H_1 < S_c$. Thus $E_{s2} \notin \Sigma_2 \subset \Omega_2$, while the sliding mode Σ_3 does not exist. Furthermore, E_{s4} becomes a pseudoequilibrium. Then we have the following result.

Theorem 5.1. *E_{s4} is globally asymptotically stable if $S_4^* < S_c < S_3^*$ and*

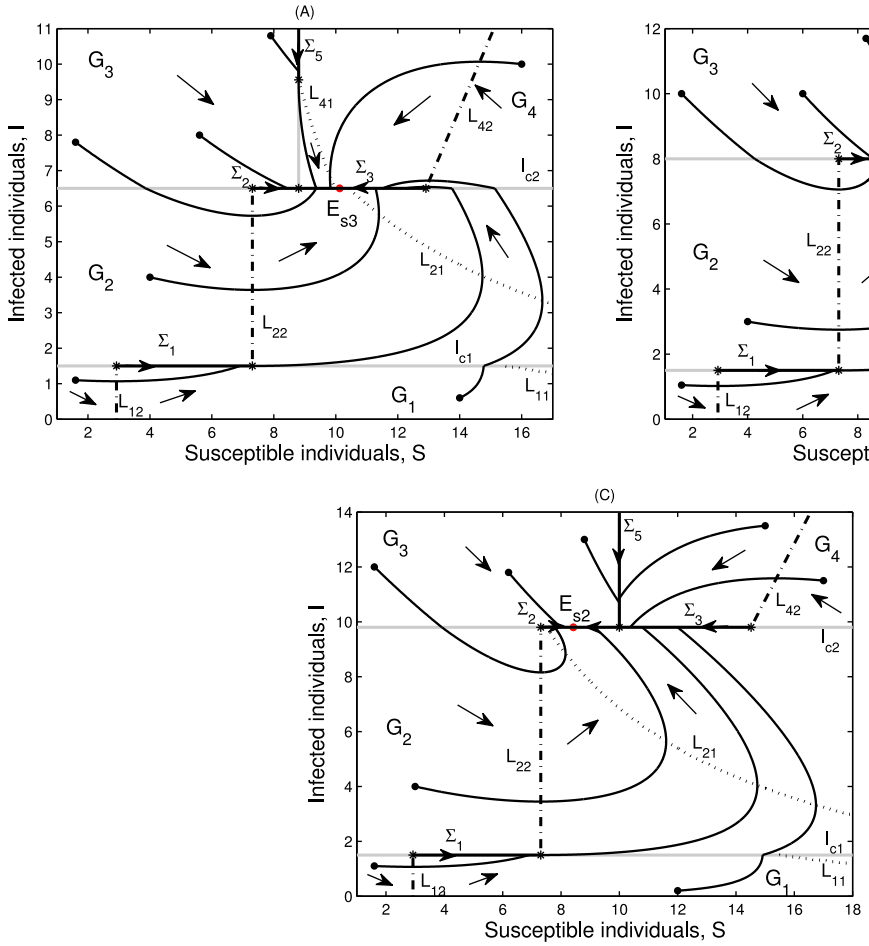

Fig. 9. Basic behaviour of solutions of system (2.1)–(2.2) in Case B.12. For (A), we choose $S_c = 8.8$, $I_{c_1} = 1.5$ and $I_{c_2} = 6.5$ such that $E_{s2} \notin \Sigma_2 \subset \Omega_2$, $E_{s3} \in \Sigma_3 \subset \Omega_2$. For (B), we choose $S_c = 10$, $I_{c_1} = 1.5$ and $I_{c_2} = 8$ such that $E_{s2} \notin \Sigma_2 \subset \Omega_2$, $E_{s3} \notin \Sigma_3 \subset \Omega_2$. For (C), we choose $S_c = 10$, $I_{c_1} = 1.5$ and $I_{c_2} = 9.8$ such that $E_{s2} \in \Sigma_2 \subset \Omega_2$, $E_{s3} \notin \Sigma_3 \subset \Omega_2$.

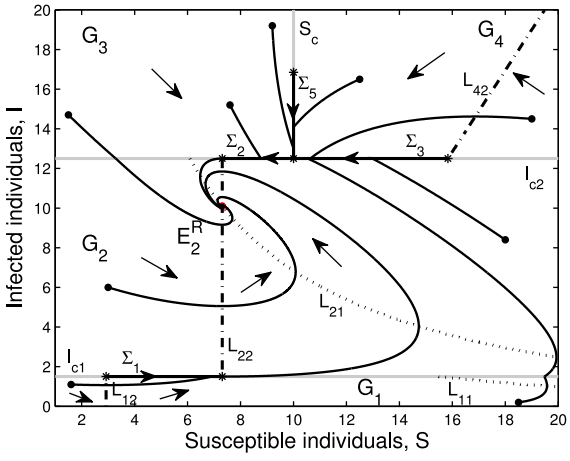

Fig. 10. E_2^R is globally asymptotically stable in Case B.13, where $S_c = 10$, $I_{c_1} = 1.5$ and $I_{c_2} = 12.5$.

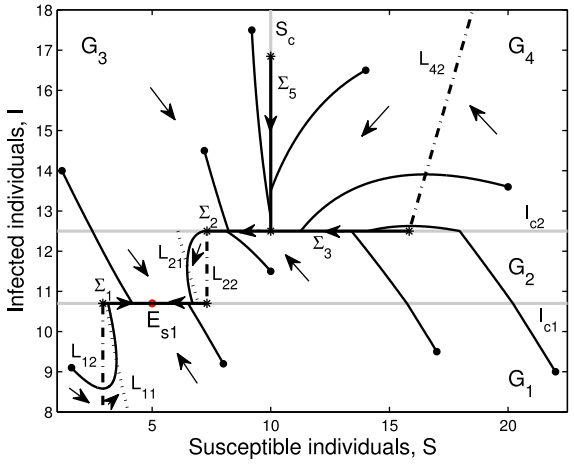

Fig. 11. E_{s1} is globally asymptotically stable in Case B.31, where $S_c = 10$, $I_{c_1} = 10.7$ and $I_{c_2} = 12.5$.

$I_{c_1} < I_{c_2} < I_4^*$.

Fig. 13 shows the phase portrait of this case. All trajectories will converge to E_{s4}.

5.1.2. Case C.12: $I_4^* < I_{c_2} < I_2^*$

Under these conditions, E_2 is a virtual equilibrium, denoted by E_2^V. The equivalent relations between I_{c_2} and I_{s4}^* can determine whether E_{s4} becomes a pseudoequilibrium or not. In this case, since $S_4^* < S_c < S_3^*$, we have $I_4^* < I_{s4}^* < I_3^* (< I_2^*)$. Then we consider two situations: $I_4^* < I_{c_2} < I_{s4}^*$ and $I_{s4}^* < I_{c_2} < I_2^*$.

Proposition 5.1. *If $I_4^* < I_{c_2} < I_{s4}^*$, then E_{s4} becomes a pseudoequilibrium, whereas $E_{s2} \notin \Sigma_2 \subset \Omega_2$ and the sliding mode Σ_3 does not exist.*

Since the exact expression of g_3 is too complicated, the equivalent relations between g_3 and I_{s4}^* cannot be determined. Thus we consider two situations: $g_3 < I_{s4}^*$ and $g_3 > I_{s4}^*$.

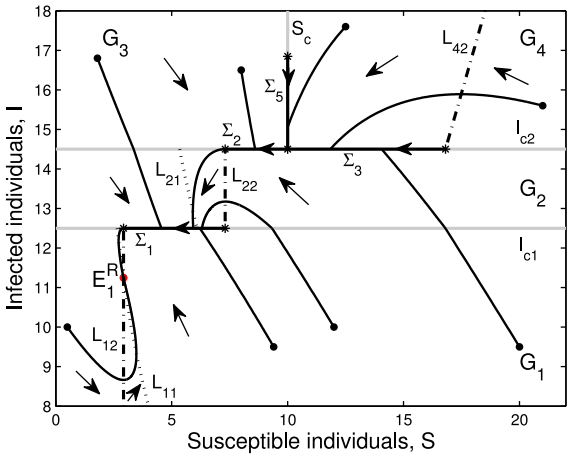

Fig. 12. E_1^R is globally asymptotically stable in Case B.41, where $S_c = 10$, $I_{c_1} = 12.5$ and $I_{c_2} = 14.5$.

Proposition 5.2. *If $I_{s4}^* < I_{c_2} < I_2^*$, then E_{s4} is not a pseudoequilibrium.*

(i) *If $I_{s4}^* < I_{c_2} < g_1$, then E_{s2} is not a pseudoequilibrium.*
- *Assume that $g_3 < I_{s4}^*$. Then E_{s3} is not a pseudoequilibrium.*
- *Assume that $g_3 > I_{s4}^*$.*
  - *If $I_{s4}^* < I_{c_2} < g_3$, then E_{s3} is a pseudoequilibrium.*
  - *If $g_3 < I_{c_2} < g_1$, then E_{s3} is not a pseudoequilibrium.*

(ii) *If $g_1 < I_{c_2} < I_2^*$, then E_{s2} is a pseudoequilibrium, whereas E_{s3} is not a pseudoequilibrium.*

The phase portrait for Proposition 5.1 is relatively similar to Fig. 13 and is not given here. Then, from Proposition 5.2, there are three situations, as displayed in Fig. 14. First, from Fig. 14(A), we see that $E_{s2} \notin \Sigma_2 \subset \Omega_2$ and $E_{s3} \notin \Sigma_3 \subset \Omega_2$; that is, no equilibrium exists in system (2.1)–(2.2). Thus all solutions will converge to the pseudoattractor $E_c = (S_c, I_{c2})$. E_{s2} is the unique globally asymptotically stable equilibrium on $\Sigma_2 \subset \Omega_2$, so all trajectories will converge to E_{s2}, as shown in Fig. 14(B). Finally, system (2.1)–(2.2) has a unique globally asymptotically stable equilibrium E_{s3} on $\Sigma_3 \subset \Omega_2$, so all trajectories will approach E_{s3}, as represented in Fig. 14(C).

5.1.3. Case C.13: $I_{c_2} > I_2^*$

Under these conditions, E_2 is a real equilibrium, whereas E_4 is a virtual equilibrium, denoted by E_2^R and E_4^V, respectively. Since $I_{c_2} > I_2^* > I_{s4}^*$, we have $H_1 > S_c$. Then E_{s2}, E_{s3} and E_{s4} are not pseudo equilibria. We obtain the following result.

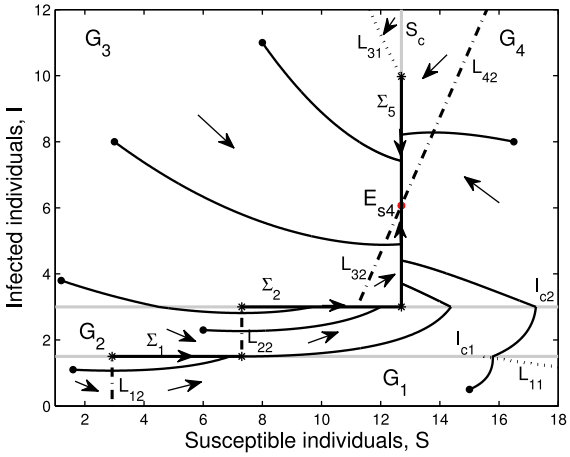

Fig. 13. E_{s4} is globally asymptotically stable in Case C.11, where $S_c = 12.7$, $I_{c_1} = 1.5$ and $I_{c_2} = 3$.

Theorem 5.2. *E_2^R is globally asymptotically stable if $S_4^* < S_c < S_3^*$, $I_{c_1} < I_4^*$ and $I_{c_2} > I_2^*$.*

The phase portrait for this case is shown in Fig. 15. All trajectories will approach E_2^R.

5.2. Case C.2: $I_4^* < I_{c_1} < I_2^*$

In this case, for the situation $I_4^* < I_{c_1} < I_{c_2} < I_2^*$, the analysis is similar to Case C.12 and is not given here; for the situation $I_{c_2} > I_2^*$, the discussion is similar to Case C.13 and is omitted here.

5.3. Case C.3: $I_2^* < I_{c_1} < I_1^*$

In this case, E_1 and E_2 are virtual equilibria, denoted by E_1^V and E_2^V, respectively. Moreover, E_{s1} is a pseudoequilibrium on $\Sigma_1 \subset \Omega_1$.

5.3.1. Case C.31: $I_{c_2} > I_{c_1} > I_2^*$

Since $I_{c_2} > I_2^* > I_{s4}^*$, we have $H_1 > S_c$. Then E_{s2}, E_{s3} and E_{s4} are not pseudoequilibria. So E_{s1} is the unique equilibrium. We thus have the following result.

Theorem 5.3. *E_{s1} is globally asymptotically stable if $S_4^* < S_c < S_3^*$, $I_2^* < I_{c_1} < I_1^*$ and $I_{c_2} > I_{c_1} > I_2^*$.*

The phase portrait for this case is shown in Fig. 16. All solutions will converge to E_{s1}.

5.4. Case C.4: $I_{c_1} > I_1^*$

In this case, E_1 is a real equilibrium, whereas E_2 is a virtual equilibrium. We denote them E_1^R and E_2^V, respectively. Moreover, $E_{s1} \notin \Sigma_1 \subset \Omega_1$.

5.4.1. Case C.41: $I_{c_2} > I_{c_1} > I_1^*$

Since $I_{c_2} > I_1^* > I_{s4}^*$, we have $H_1 > S_c$. Thus E_{s2}, E_{s3} and E_{s4} are not pseudoequilibria. Furthermore, E_1^R is the unique equilibrium. Then we have the following result.

Theorem 5.4. *E_1^R is globally asymptotically stable if $S_4^* < S_c < S_3^*$ and $I_{c_2} > I_{c_1} > I_1^*$.*

Fig. 17 shows the phase portrait of this case. All solutions will converge to E_1^R.

6. Global behaviour in Case D: $S_c > S_3^*$

For Case D, E_4 is a virtual equilibrium, denoted by E_4^V. Since $S_c > S_3^*$, we have $I_{s4}^* > I_3^*$, $g_2 < I_4^*$ and $g_2 < g_1 < I_3^*$. The investigations of the sliding mode on Σ_2 and Σ_3, as well as the existence of pseudoequilibria E_{s2} and E_{s3} are similar to Proposition 4.1. In addition, from Proposition 2.5, there may exist a sliding domain Σ_5 on Ω_3; however, E_{s4} is never a pseudoequilibrium on $\Sigma_5 \subset \Omega_3$.

Next, E_1, E_2 or E_3 may be real, and E_{s1}, E_{s2} or E_{s3} may become pseudoequilibria, depending on the values of the infected threshold I_{c_1} and I_{c_2}.

6.1. Case D.1: $I_{c_1} < I_3^*$

In this case, E_1 is a virtual equilibrium, denoted by E_1^V. Furthermore, $E_{s1} \notin \Sigma_1 \subset \Omega_1$.

6.1.1. Case D.11: $I_{c_1} < I_{c_2} < I_3^*$

Under these conditions, E_2 is a virtual equilibrium, whereas E_3 is a real equilibrium. We denote them E_2^V and E_3^R, respectively. Note that $I_{c_2} < I_3^* < I_{s4}^*$, so we have $S_c > H_1$. Therefore E_{s2} is not a pseudo equilibrium on $\Sigma_2 \subset \Omega_2$, while the sliding mode Σ_3 does not exist. Thus we have the following.

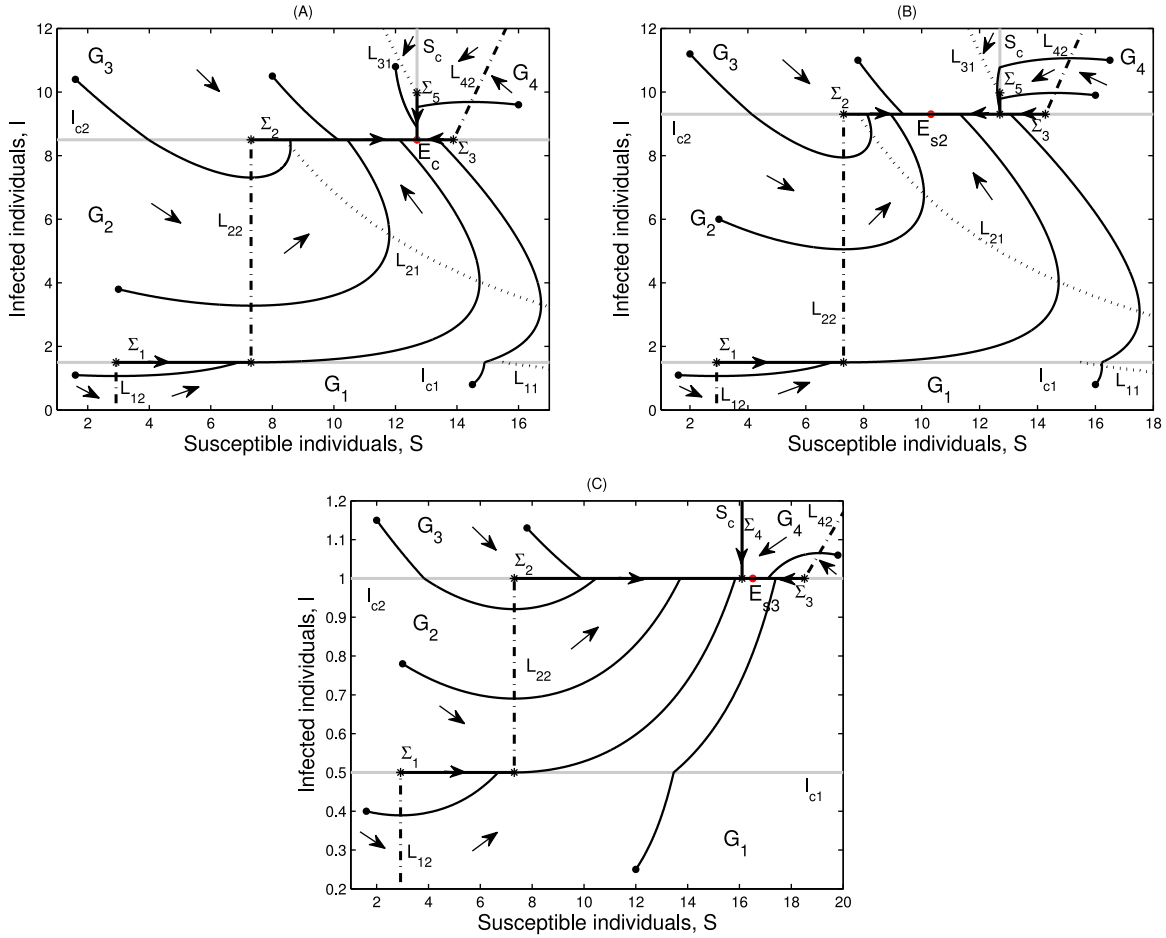

Fig. 14. Basic behaviour of solutions of system (2.1)–(2.2) in Case C.12. For (A), we choose $S_c = 12.7$, $I_{c_1} = 1.5$ and $I_{c_2} = 8.5$ such that $E_{s2} \notin \Sigma_2 \subset \Omega_2$, $E_{s3} \notin \Sigma_3 \subset \Omega_2$. For (B), we choose $S_c = 12.7$, $I_{c_1} = 1.5$ and $I_{c_2} = 9.3$ such that $E_{s2} \in \Sigma_2 \subset \Omega_2$, $E_{s3} \notin \Sigma_3 \subset \Omega_2$. For (C), we choose all parameter values the same as other cases except $h = 0.9$, and $S_c = 16.1$, $I_{c_1} = 0.5$, $I_{c_2} = 1$ such that $E_{s2} \notin \Sigma_2 \subset \Omega_2$, $E_{s3} \in \Sigma_3 \subset \Omega_2$.

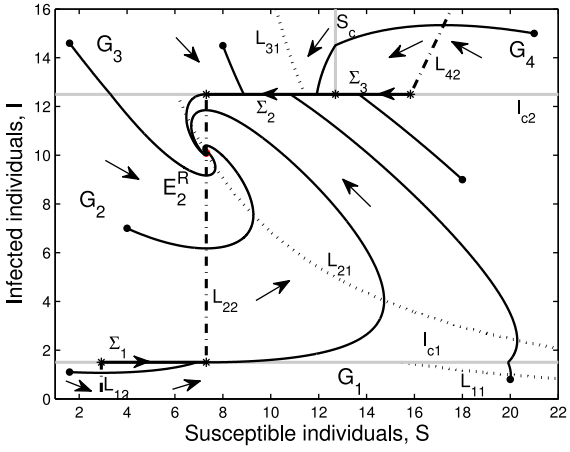

Fig. 15. E_2^R is globally asymptotically stable in Case C.13, where $S_c = 12.7$, $I_{c_1} = 1.5$ and $I_{c_2} = 12.5$.

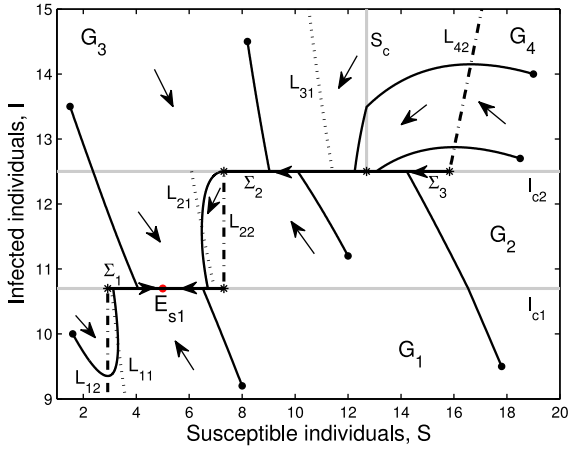

Fig. 16. E_{s1} is globally asymptotically stable in Case C.31, where $S_c = 12.7$, $I_{c_1} = 10.7$ and $I_{c_2} = 12.5$.

Theorem 6.1. *E_3^R is globally asymptotically stable if $S_c > S_3^*$ and $I_{c_1} < I_{c_2} < I_3^*$.*

The phase portrait is shown in Fig. 18. All solutions will converge to E_3^R as time t increases.

6.1.2. Case D.12: $I_3^* < I_{c_2} < I_2^*$

Under these conditions, both E_2 and E_3 are virtual equilibria, denoted by E_2^V and E_3^V, respectively. Meanwhile, note that $g_1 < I_3^* < I_{s4}^*$, so we have $g_3 < I_{s4}^*$. Since the equivalent relations between I_2^* and I_{s4}^* cannot be determined, we consider two situations: $I_2^* < I_{s4}^*$ and $I_2^* > I_{s4}^*$.

Proposition 6.1. *Suppose that $I_2^* < I_{s4}^*$. Then $H_1 < S_c$. Thus $E_{s2} \in \Sigma_2 \subset \Omega_2$, while the sliding domain Σ_3 does not exist.*

Proposition 6.2. *Suppose that $I_{s4}^* < I_2^*$.*

(i) *If $I_3^* < I_{c_2} < I_{s4}^*$, we have $S_3^* < H_1 < S_c$. Then $E_{s2} \in \Sigma_2 \subset \Omega_2$, whereas*

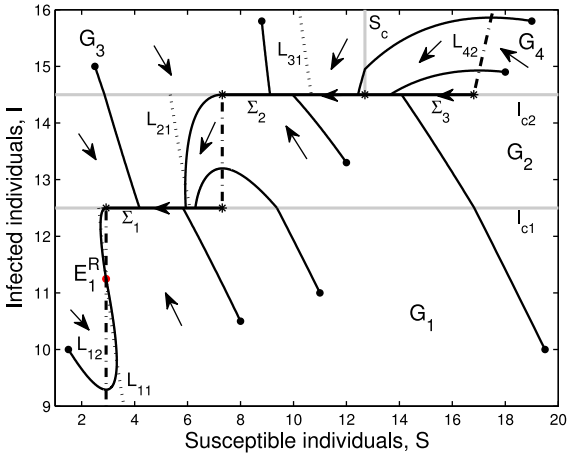

Fig. 17. E_1^R is globally asymptotically stable in Case C.41, where $S_c = 12.7$, $I_{c_1} = 12.5$ and $I_{c_2} = 14.5$.

Σ_3 *does not exist.*

(ii) *If* $I_{s4}^* < I_{c_2} < I_2^*$, *we have* $H_1 > S_c$. *Then* $E_{s2} \in \Sigma_2 \subset \Omega_2$, $E_{s3} \notin \Sigma_3 \subset \Omega_2$.

Therefore, from Propositions 6.1 and 6.2, we see that E_{s2} is the unique equilibrium for system (2.1) with (2.2), which is globally asymptotically stable. Additionally, the phase portrait of this case is shown in Fig. 19. All trajectories will converge to E_{s2}.

6.1.3. Case D.13: $I_{c_2} > I_2^*$

Under these conditions, E_2 is a real equilibrium, whereas E_3 is a virtual equilibrium. We denote them E_2^R and E_3^V, respectively. However, the equivalent relations between I_2^* and I_{s4}^* cannot be determined, so we consider two situations: $I_2^* < I_{s4}^*$ and $I_2^* > I_{s4}^*$.

Proposition 6.3. *Suppose that* $I_2^* > I_{s4}^*$. *Then* $H_1 > S_c$. *Thus* E_{s2} *and* E_{s3} *are not pseudoequilibria.*

Proposition 6.4. *Suppose that* $I_{s4}^* > I_2^*$.

(i) *If* $I_2^* < I_{c_2} < I_{s4}^*$, *we have* $H_1 < S_c$. *Then* $E_{s2} \notin \Sigma_2 \subset \Omega_2$, *whereas* Σ_3 *does not exist.*

(ii) *If* $I_{c_2} > I_{s4}^*$, *we have* $H_1 > S_c$. *Then* E_{s2} *and* E_{s3} *are not pseudo equilibria.*

Therefore, from Propositions 6.3 and 6.4, we see that E_2^R is the unique globally asymptotically stable equilibrium for system (2.1)–(2.2). Fig. 20 represents the phase portrait of this case. All orbits will converge to E_2^R.

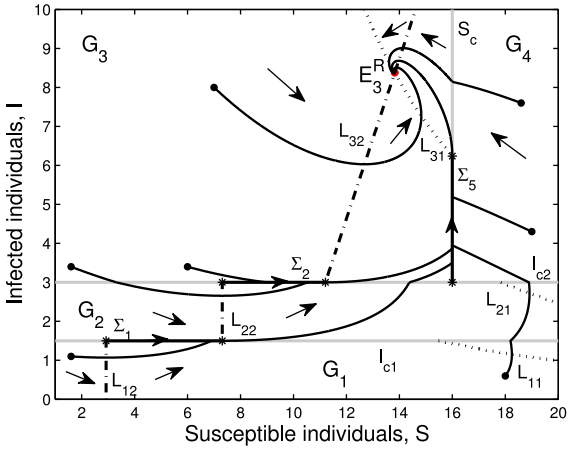

Fig. 18. E_3^R is globally asymptotically stable in Case D.11, where $S_c = 16$, $I_{c_1} = 1.5$ and $I_{c_2} = 3$.

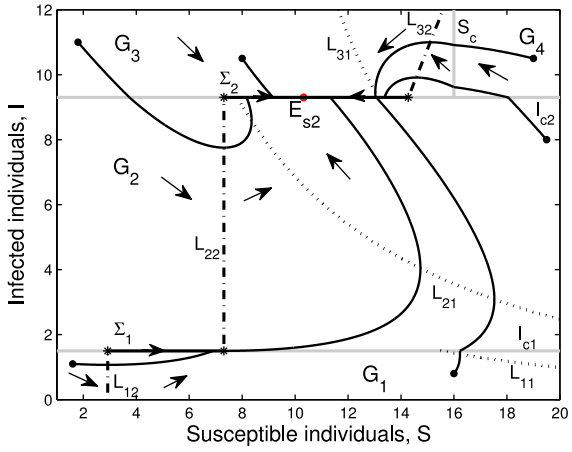

Fig. 19. E_{s2} is globally asymptotically stable in Case D.12, where $S_c = 16$, $I_{c_1} = 1.5$ and $I_{c_2} = 9.3$.

6.2. Case D.2: $I_3^* < I_{c_1} < I_2^*$

In this case, for the situation $I_4^* < I_{c_1} < I_{c_2} < I_2^*$, the analysis is similar to Case D.12 and is not given here; for the situation $I_{c_2} > I_2^*$, the discussion is similar to Case D.13 and is omitted here.

6.3. Case D.3: $I_2^* < I_{c_1} < I_1^*$

In this case, E_1, E_2 and E_3 are virtual equilibria, denoted by E_1^V, E_2^V and E_3^V, respectively. Moreover, E_{s1} is a pseudoequilibrium on $\Sigma_1 \subset \Omega_1$.

6.3.1. Case D.31: $I_{c_2} > I_{c_1} > I_2^*$

A similar discussion can be found in Propositions 6.3 and 6.4. We have $E_{s2} \notin \Sigma_2 \subset \Omega_2$. The sliding domain Σ_3 may not exist, while if Σ_3 exists, E_{s3} is never a pseudoequilibrium. Therefore E_{s1} is the unique equilibrium for system (2.1)–(2.2). Then we have the following result.

Theorem 6.2. E_{s1} *is globally asymptotically stable if* $S_c > S_3^*$, $I_2^* < I_{c_1} < I_1^*$ *and* $I_{c_2} > I_{c_1} > I_2^*$.

The phase portrait for this case is displayed in Fig. 21. All trajectories will approach E_{s1}.

6.4. Case D.4: $I_{c_1} > I_1^*$

In this case, E_1 is a real equilibrium, whereas E_2 and E_3 are virtual equilibria, denoted by E_1^R, E_2^V and E_3^V, respectively. Moreover, $E_{s1} \notin \Sigma_1 \subset \Omega_1$.

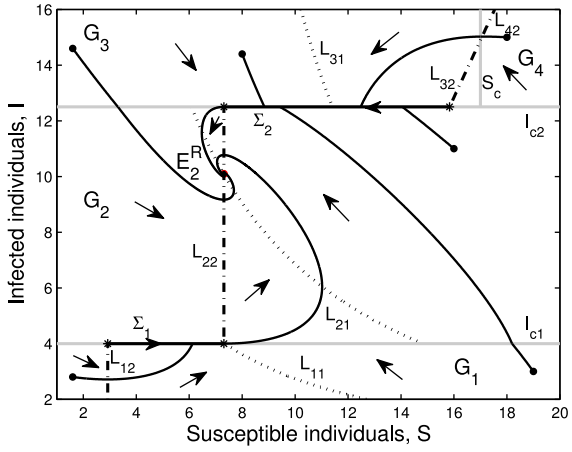

Fig. 20. E_2^R is globally asymptotically stable in Case D.13, where $S_c = 17$, $I_{c_1} = 4$ and $I_{c_2} = 12.5$.

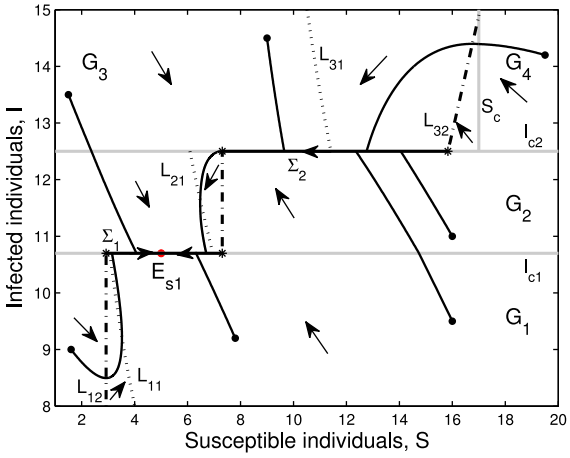

Fig. 21. E_{s1} is globally asymptotically stable in Case D.31, where $S_c = 17$, $I_{c_1} = 10.7$ and $I_{c_2} = 12.5$.

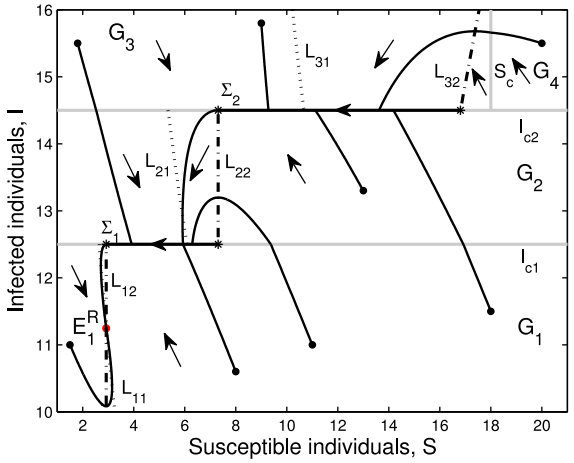

Fig. 22. E_1^R is globally asymptotically stable in Case D.41, where $S_c = 18$, $I_{c_1} = 12.5$ and $I_{c_2} = 14.5$.

6.4.1. Case D.41: $I_{c_2} > I_{c_1} > I_1^*$

From Propositions 6.3 and 6.4, we have $E_{s2} \notin \Sigma_2 \subset \Omega_2$. The sliding domain Σ_3 may not exist, and even if Σ_3 exists, E_{s3} is not a pseudo equilibrium. Thus E_1^R is the unique equilibrium for system (2.1)–(2.2). Then we have the following result.

Theorem 6.3. *E_1^R is globally asymptotically stable if $S_c > S_3^*$ and $I_{c_2} > I_{c_1} > I_1^*$.*

The phase portrait for this case is displayed in Fig. 22. All orbits will converge to E_1^R.

7. Discussion

Only a handful of Filippov models have been formulated to describe the impact of media coverage and quarantine of susceptible individuals on the transmission dynamics of human influenza [20,34,35]. In general, these proposed models consider that the general public and the mass media are usually not aware of the disease when the number of infected individuals is relatively small, while once the number of patients exceeds a certain infected threshold value, media reports begin to exhibit their effects. We have modelled the effect of individuals' behaviour changing because of media coverage, which consequently changes the way of influenza transmission. That is, when the number of infected individuals becomes larger, the transmission between infected and susceptible individuals tends to a saturation level due to the protection measures taken by the general public. To model this, we described the incidence rate with a saturated function to represent saturation effects once the number of infected individuals exceeds another larger infected threshold level I_{c_2}. Additionally, when the case number exceeds this larger infected threshold value, in order to reduce the spread of influenza and the socioeconomic costs, we quarantined susceptible individuals if the number of susceptible individuals is larger than a threshold value. Therefore the Filippov model (2.1)–(2.2) constructed here can be used to describe this more realistic impact of media coverage and quarantine (of susceptible individuals) on influenza.

We investigated the global property of the Filippov system (2.1)–(2.2) with regard to the existence and stability of all possible equilibria and sliding-mode dynamics. Different values of the thresholds S_c, I_{c_1} and I_{c_2} were chosen to exhibit various dynamic behaviours. We summarize the main results in Table 2 associated with their corresponding biological outcomes as follows.

(I) If the infected threshold value I_{c_2} ($> I_{c_1}$) is sufficiently low, then the number of infected individuals will rise above I_{c_2} to reach the level of a globally asymptotically stable equilibrium (E_4^R or E_{s4} or E_3^R), regardless of the susceptible threshold value S_c, as shown in Figs. 3, 8, 13 and 18. Thus it is impossible to avoid an influenza outbreak.

(II) For these choices of S_c, I_{c_1} and I_{c_2}, all orbits of system (2.1)–(2.2) will converge to either the pseudoequilibrium on $I = I_{c_2}$ (E_{s2} or E_{s3}) or the pseudoattractor $E_c = (S_c, I_{c_2})$, as displayed in Figs. 4, 9, 14 and 19. Thus the number of infected individuals will eventually stabilize at a level equal to I_{c_2}.

(III) For these cases, all trajectories of system (2.1)–(2.2) will converge to the globally asymptotically stable equilibrium E_2^R that lies between I_{c_1} and I_{c_2} (see Figs. 5, 10, 15 and 20). Since the infected level will eventually stabilize at a level in between I_{c_1} and I_{c_2}, there is an epidemic for this situation.

(IV) In these situations, system (2.1)–(2.2) has a unique globally asymptotically stable pseudoequilibrium E_{s1} on $I = I_{c_1}$ or a unique globally asymptotically stable equilibrium E_1^R that lies below I_{c_1}. So the number of infected individuals will eventually stabilize at a level below or equal to I_{c_1}, as represented in Figs. 6, 7, 11, 12, 16, 17, 21 and 22. Therefore, our control objective — reducing the number of infected individuals below or equal to the smaller infected threshold value I_{c_1} — can be achieved eventually.

Fig. 23 illustrates the main results in graphical form. We can also calculate the relative sizes of the equilibrium components. From the mathematical expressions of the endemic equilibria $E_i = (S_i^*, I_i^*)$, $i = 1, 2, 3, 4$, we see that $S_1^* = \frac{\mu+\alpha+\gamma}{\beta}$, $S_2^* = \frac{\mu+\alpha+\gamma}{\beta(1-\epsilon_1)}$, $S_3^* = \frac{\Lambda h+\mu+\alpha+\gamma}{\beta(1-\epsilon_2)+\mu h}$ and $S_4^* = \frac{\Lambda h+\mu+\alpha+\gamma}{\beta(1-\epsilon_2)+(\mu+q)h}$. After direct calculations, we have $S_1^* < S_2^* < S_4^* < S_3^*$. In a similar way, we also have $I_1^* > I_2^* > I_3^* > I_4^*$.

It can be seen from the above conclusions that the Filippov system eventually converges to the endemic equilibrium E_i^R, the pseudo equilibrium E_{si} or the pseudoattractor $E_c = (S_c, I_{c_2})$, for $i = 1, 2, 3, 4$, depending on the choices of the threshold values S_c, I_{c_1} and I_{c_2}. This implies that the choices of the susceptible and infected threshold values are of great significance. For Case (I), if the infected threshold value I_{c_2} is chosen sufficiently small, then taking control strategies may waste a lot of resources. In fact, the susceptible and infected threshold values should be chosen appropriately, neither too large or too small. Furthermore, for Cases (II) and (III), human influenza becomes an epidemic, since the infected number stabilizes at a level in between I_{c_1} and I_{c_2}. Additionally, our aim — ensuring the number of infected individuals remains either below or at a previously given level (I_{c_1}) — can be achieved for Case (IV). Therefore our findings could be beneficial for policymakers to choose appropriate threshold values and take control strategies accordingly.

Table 2
Main results of system (2.1)–(2.2), where $I_{c_2} > I_{c_1}$.

Tolerance thresholds	$S_c < S_2^*$	$S_2^* < S_c < S_4^*$	$S_4^* < S_c < S_3^*$ ($I_4^* < I_{s4}^* < I_3^*$)	$S_c > S_3^*$
	$I_{c_2} < I_4^*$: (I)	$I_{c_2} < I_4^*$: (I)	$I_{c_2} < I_{s4}^*$: (I)	$I_{c_2} < I_3^*$: (I)
$I_{c_1} < I_2^*$	$I_4^* < I_{c_2} < I_2^*$: (II)	$I_4^* < I_{c_2} < I_2^*$: (II)	$I_{s4}^* < I_{c_2} < I_2^*$: (II)	$I_3^* < I_{c_2} < I_2^*$: (II)
	$I_{c_2} > I_2^*$: (III)	$I_{c_2} > I_2^*$: (III)	$I_{c_2} > I_2^*$: (III)	$I_{c_2} > I_2^*$: (III)
$I_2^* < I_{c_1} < I_1^*$	$I_{c_2} > I_2^*$: (IV)	$I_{c_2} > I_2^*$: (IV)	$I_{c_2} > I_2^*$: (IV)	$I_{c_2} > I_2^*$: (IV)
$I_{c_1} > I_1^*$	$I_{c_2} > I_1^*$: (IV)	$I_{c_2} > I_1^*$: (IV)	$I_{c_2} > I_1^*$: (IV)	$I_{c_2} > I_1^*$: (IV)

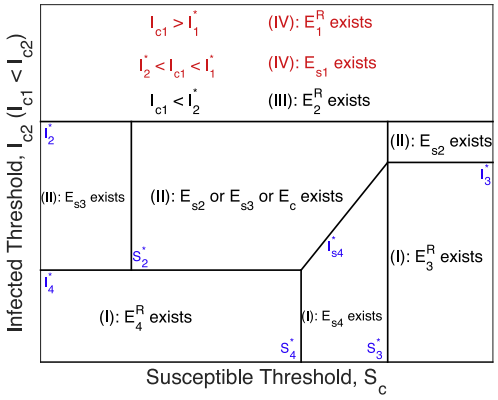

Fig. 23. Summary of the main results.

An advantage of our results over other existing work is that we were able to prove global stability in a large number of cases. This was done by excluding the existence of limit cycles and using a modified Dulac function that avoids the sliding modes.

This study is a preliminary exploration of the impact of media coverage and quarantine (of susceptible individuals) on the transmission of human influenza and could be improved in several ways. Note that the media function induced by both the case number (I) and significant changes in the number of cases (dI/dt) could also affect the size of an influenza outbreak or the peak time. Thus more elaborate forms of the media-coverage function would be proposed in the mathematical models. For example, media/psychological impact, as awareness of the presence of influenza, could be described by an exponentially decreasing function, resulting in the transmission rate $\beta e^{-M(I,dI/dt)}$, where $M(I, dI/dt) = \max\{0, q_1 I(t) + q_2 \frac{dI(t)}{dt}\}$ and q_1 and q_2 are non-negative parameters to measure the effects of media. We leave these for future investigation.

Acknowledgments

CC acknowledges support from China Scholarship Council Programs. NSC acknowledges support from the Ministry of Higher Education, Malaysia, and the School of Informatics and Applied Mathematics, Universiti Malaysia Terengganu. RS? is supported by an NSERC Discovery Grant. For citation purposes, please note that the question mark in “Smith?” is part of his name.

References

[1] R.G. Webster, The importance of animal influenza for human disease, Vaccine 20 (2002) S16–S20.
[2] D. Kumar, S. Broor, M.S. Rajala, Interaction of host nucleolin with influenza A virus nucleoprotein in the early phase of infection limits the late viral gene expression, PLoS One 11 (2016) e0164146.
[3] World Health Organization (WHO), World now at the start of 2009 influenza pandemic, Available: http://www.who.int/mediacentre/news/statements/2009/h1n1_pandemic_phase6_20090611/en/, 2009.
[4] M. Richard, M. Graaf de, S. Herfst, Avian influenza A viruses: from zoonosis to pandemic, Future Virol. 9 (2014) 513–524.
[5] A. Kandeel, P. Dawson, M. Labib, M. Said, S. El-Refai, A. El-Gohari, M. Talaat, Morbidity, mortality, and seasonality of influenza hospitalizations in Egypt, November 2007-November 2014, PLoS One 11 (2016) e0161301.
[6] J.W. McCauley, S. Hongo, N.V. Kaverin, G. Kochs, R.A. Lamb, et al., Family Orthomyxoviridae. Virus Taxonomy, in: A.M.Q. King, M.J. Adams, E.B. Carstens, E.J. Lefkowitz (Eds.), Ninth Report of the International Committee on Taxonomy of Viruses, Amsterdam: Elsevier, 2012, pp. 749–761.
[7] A.J. Hay, V. Gregory, A.R. Douglas, Y.P. Lin, The evolution of human influenza viruses, Phil. Trans. R. Soc. London B 356 (2001) 1861–1870.
[8] Y.Q. Wang, J.X. Qu, Q. Ba, J.H. Dong, et al., Detection and typing of human-infecting influenza viruses in China by using a multiplex DNA biochip assay, J. Virol. Methods 234 (2016) 178–185.
[9] S. Tong, X. Zhu, Y. Li, M. Shi, J. Zhang, et al., New world bats harbor diverse influenza A viruses, PLoS Pathog. 9 (2013) e1003657.
[10] J.Q. Zhao, J.K. Liu, S.V. Vemula, C. Lin, J.Y. Tan, V. Ragupathy, X. Wang, et al., Sensitive detection and simultaneous discrimination of influenza A and B viruses in nasopharyngeal swabs in a single assay using next-generation sequencing-based diagnostics, PLoS One 11 (2016) e0163175.
[11] R. Gao, B. Cao, Y. Hu, Z. Feng, D. Wang, et al., Human infection with a novel avian-origin influenza A (H7N9) virus, N. Engl. J. Med. 368 (2013) 1888–1897.
[12] W.D. Tanner, D.J.A. Toth, A.V. Gundlapalli, The pandemic potential of avian influenza A(H7N9) virus: a review, Epidemiol. Infect. 143 (2015) 3359–3374.
[13] J. Parry, WHO investigates possible human to human transmission of avian flu, BMJ (Clin.Res. ed) 328 (2004) 7435.
[14] X. Qi, Y.H. Qian, C.J. Bao, X.L. Guo, L.B. Cui, F.Y. Tang, et al., Probable person to person transmission of novel avian influenza A (H7N9) virus in eastern China, 2013: epidemiological investigation, BMJ 347 (2013) f4752.
[15] J.W. Rudge, R. Coker, Human to human transmission of H7N9, BMJ 347 (2013) f4730.
[16] M. Linster, S. van Boheemen, M. de Graaf, et al., Identification, characterization, and natural selection of mutations driving airborne transmission of A/H5N1 virus, Cell 157 (2014) 329–339.
[17] J. Peng, H. Yang, H. Jiang, Y.X. Lin, C.D. Lu, Y.W. Xu, J. Zeng, The origin of novel avian influenza A H7N9 and mutation dynamics for its human-to-human transmissible capacity, PLoS One 9 (2014) e93094.
[18] F.B. Agusto, Optimal isolation control strategies and cost-effectiveness analysis of a two-strain avian influenza model, BioSystems 113 (2013) 155–164.
[19] J.J. Reynolds, M. Torremorell, M.E. Craft, Mathematical modeling of influenza A virus dynamics within swine farms and the effects of vaccination, PLoS One 9 (2014) e106177.
[20] N.S. Chong, R.J. Smith?, Modelling avian influenza using Filippov systems to determine culling of infected birds and quarantine, Nonlinear Anal. Real World Appl. 24 (2015) 196–218.
[21] K.W. Chung, R. Lui, Dynamics of two-strain influenza model with cross-immunity and no quarantine class, J. Math. Biol. 73 (2016) 1467–1489.
[22] J.M. Tchuenche, N. Dube, C.P. Bhunu, R.J. Smith?, C.T. Bauch, The impact of media coverage on the transmission dynamics of human influenza, BMC Public Health 11 (2011) S5.
[23] S.H. Liu, L.Y. Pang, S.G. Ruan, X.N. Zhang, Global dynamics of avian influenza epidemic models with psychological effect, Comput. Math. Method M 2015 (2015). Article ID 913726.
[24] Q.L. Yan, S.Y. Tang, S. Gabriele, J.H. Wu, Media coverage and hospital notifications: Correlation analysis and optimal media impact duration to manage a pandemic, J. Theor. Biol. 390 (2016) 1–13.
[25] L. Mitchell, J.V. Ross, A data-driven model for influenza transmission incorporating media effects, R. Soc. Open Sci. 3 (2016) 160481.
[26] Y.N. Xiao, S.Y. Tang, J.H. Wu, Media impact switching surface during an infectious disease outbreak, Sci. Rep. 5 (2015) 7838.
[27] S. Collinson, K. Khan, J.M. Heffernan, The effects of media reports on disease spread and important public health measurements, PLoS One 10 (2015) e0141423.
[28] N. Tuncer, M. Martcheva, Modeling seasonality in Avian influenza H5N1, J. Biol. Syst. 21 (2013) 134004.
[29] Y.N. Xiao, X.D. Sun, S.Y. Tang, J.H. Wu, Transmission potential of the novel avian influenza A(H7N9) infection in mainland China, J. Theor. Biol. 352 (2014) 1–5.
[30] J. Zhang, J. Jin, G.Q. Sun, X.D. Sun, Y.M. Wang, B.X. Huang, Determination of original infection source of H7N9 avian influenza by dynamical model, Sci. Rep. 4 (2014) 4846.
[31] A.F. Filippov, Differential Equations with Discontinuous Righthand Sides, Kluwer Academic, Dordrecht, 1988.
[32] R.I. Leine, Bifurcations in Discontinuous Mechanical Systems of Filippov-Type, The Universiteitsdrukkerij TU Eindhoven, The Netherlands, 2000.
[33] M. Nuno, Z.L. Feng, M. Martcheva, C. Castillo-Chavez, Dynamics of two-strain

influenza with isolation and partial cross-immunity, SIAM J. Appl. Math. 65 (2005) 964–982.
[34] N.S. Chong, B. Dionne, R.J. Smith?, An avian-only Filippov model incorporating culling of both susceptible and infected birds in combating avian influenza, J. Math. Biol. 73 (2016) 751–784.
[35] A.L. Wang, Y.N. Xiao, A Filippov system describing media effects on the spread of infectious diseases, Nonlinear Anal. Hybrid Syst. 11 (2014) 84–97.